European Journal of Taxonomy 559: 1–37
https://doi.org/10.5852/ejt.2019.559
ISSN 2118-9773
www.europeanjournaloftaxonomy.eu
2019 · Obert T. & Vďačný P.

Research article

urn:lsid:zoobank.org:pub:8DC07412-8619-4A03-B524-04019880B9D6

Integrative taxonomy of five astome ciliates (Ciliophora, Astomatia) isolated from earthworms in Central Europe

Tomáš OBERT[1] & Peter VĎAČNÝ[2,*]

[1,2]Department of Zoology, Comenius University in Bratislava, 842 15 Bratislava, Slovakia.

[*]Corresponding author: peter.vdacny@uniba.sk
[1]Email: tomasobert.obert@gmail.com

[1]urn:lsid:zoobank.org:author:DBA6C599-9060-46FE-93CD-FE157754186B
[2]urn:lsid:zoobank.org:author:47A28E80-E04F-40C4-93A3-F7F685C9533A

Abstract. Four earthworm species, the endogeic *Octolasion tyrtaeum* (Savigny, 1826), the anecic *Lumbricus terrestris* Linnaeus, 1758 as well as the epigeic *Eisenia fetida* (Savigny, 1826) and *Dendrobaena veneta* (Rosa, 1886), were examined for the presence of astome ciliates. Based on the integrative taxonomic approach, five ciliate species were recognized in their gastrointestinal tracts: *Metaradiophrya lumbrici* (Dujardin, 1841), *M. varians* (de Puytorac, 1954), *Anoplophrya lumbrici* (Schrank, 1803), *A. vulgaris* de Puytorac, 1954 and *A. nodulata* (Dujardin, 1841). Their distinctness was assessed using the multivariate morphometric approach and molecular phylogenetic analyses. Although the two species of *Metaradiophrya* Jankowski, 2007 on the one hand and the two former species of *Anoplophrya* Stein, 1860 on the other, were not distinctly separated by the multivariate morphometric analyses, they were clearly delimited by the 18S rRNA gene sequences. Species within each genus also differed by their hosts, *M. lumbrici* and *A. lumbrici* occurred only in anecic earthworms while *M. varians* and *A. vulgaris* occured exclusively in epigeic earthworms. Only a single species, *A. nodulata*, was detected in endogeic earthworms. It was morphologically distinct from and did not cluster with the two other species of *Anoplophrya* but was nested within the paraphyletic assemblage containing other astomes from endogeic earthworms. This indicates that the evolution of endosymbiotic ciliates from earthworms has very likely proceeded through a specialization to various ecological groups of their host organisms.

Keywords. 18S rRNA gene, *Anoplophrya*, Lumbricidae, *Metaradiophrya*, morphometry.

Obert T. & Vďačný P. 2019. Integrative taxonomy of five astome ciliates (Ciliophora, Astomatia) isolated from earthworms in Central Europe. *European Journal of Taxonomy* 559: 1–37. https://doi.org/10.5852/ejt.2019.559

Introduction

The subclass Astomatia Schewiakoff, 1896 unites ciliates lacking cytostome, cytopharynx and all oral ciliary structures, such as paroral membrane or adoral organelles. Based on the ultrastructural and molecular data, mouthless (astome) ciliates are classified within the species-rich and highly morphologically as well as ecologically diverse class Oligohymenophorea de Puytorac *et al.*, 1974

(Lynn 2008; Fokam *et al.* 2011; Rataj & Vďačný 2018, 2019). Astomes are endosymbionts typically inhabiting the gastrointestinal tract of a huge variety of animals, ranging from turbellarians (e.g., von Siebold 1839; Schultze 1851; Kijenskij 1926; de Puytorac 1957, 1963; Sikora 1963; Corliss *et al.* 1965), mollusks (Lom 1959) and annelids (for reviews, see Cépède 1910 and de Puytorac 1954, 1969, 1972) to newts and frogs (e.g., Maupas 1879; Bush 1933, 1934; Kay 1942; McAllister *et al.* 1993; McAllister & Trauth 1996). The majority of astome ciliates has been, however, discovered in annelids including polychaetes (de Puytorac 1954; de Puytorac & Schrével 1965; Sauvadet *et al.* 2017), leeches and, especially, in a variety of aquatic and terrestrial oligochaetes (e.g., Cépède 1910; Rossolimo 1926a, 1926b; Heidenreich 1935; de Puytorac 1954, 1969, 1972; Ngassam 1983; Ngassam *et al.* 1998; Fokam *et al.* 2008, 2015, 2016).

The gastrointestinal tract of earthworms from the oligochaete family Lumbricidae Rafinesque-Schmaltz, 1815 is inhabited by astomes belonging to only three genera: *Metaradiophrya* Jankowski, 2007, *Anoplophrya* Stein, 1860 and *Maupasella* Cépède, 1910 (Heidenreich 1935; Lom 1961; de Puytorac 1972). Each genus has dozens of species and some of them have a complex taxonomic history (see, Heidenreich 1935; Beers 1938; Williams 1942; Lom 1961; de Puytorac 1972). Most taxonomic problems have arisen from the paucity of morphological differential features as well as from the lack of information on intraspecies variability and host range. Host species very likely constitute clearly isolated ecological niches that might permit speciation of symbiotic ciliates (Irwin & Lynn 2015; Irwin *et al.* 2017; Vďačný 2018; Vďačný *et al.* 2018, 2019), although no distinct apomorphic morphological features might be recognizable between astomes originated from different hosts. In this case, molecular data could independently prove the species identity and could also help to statistically delimit species boundaries (Abraham *et al.* 2019). Unfortunately, except for the study of Affa'a *et al.* (2004), molecular data are completely missing from astome ciliates isolated from lumbricid earthworms, although there are some reports from earthworms of the families Megascolecidae Rosa, 1891 and Glossoscolecidae Michaelsen, 1900 (Fokam *et al.* 2011).

Therefore, in the present study, we apply an integrative approach to study astome ciliates inhabiting the gastrointestinal tract of some lumbricid earthworms originated from Slovakia, Central Europe. Our main goals are set as follows:

1. to study the diversity and phylogeny of astome ciliates inhabiting the gastrointestinal tract of lumbricid earthworms.
2. to test the host specificity of endosymbiotic ciliates to certain ecological groups of earthworms, using 18S rRNA gene sequences.
3. to assess the morphological and genetic variability of astome ciliates isolated from lumbricid earthworms.

Material and methods

Material collection and processing

Earthworms from the family Lumbricidae were sampled at seven localities in the capital of Bratislava and in its vicinity, western Slovakia, Central Europe (Fig. 1; Table 1). Collected lumbricids were transferred together with *in situ* substrates to the laboratory at the Department of Zoology, Comenius University in Bratislava. Their identification was based on morphological characters and followed the monograph of Pižl (2002). In total, four earthworm species were determined: *Lumbricus terrestris* Linnaeus, 1758, *Eisenia fetida* (Savigny, 1826), *Dendrobaena veneta* (Rossa, 1886) and *Octolasion tyrtaeum* (Savigny, 1826). After identification, earthworms were euthanized in formalin (37%) vapors, their guts were dissected and their contents were extracted with a micropipette and observed under an optical microscope Leica DM2500. Ciliate endosymbionts were manually isolated from the gut content

with the aid of Pasteur micropipettes adjusted as described by Foissner (2014). Living ciliates were investigated at low (50–400´) and high (1000´, oil immersion) magnifications, using bright field and differential interference contrast optics (Foissner 2014). Images were captured by a Canon EOS 70D camera. Ciliates were measured from images, using the calibrated software ImageJ ver. 1.49 (Schneider *et al.* 2012).

Multivariate taxonomic methods

A multivariate approach was used to investigate the morphometric variation and distinctness of four astome species isolated from the gastrointestinal tract of earthworms. Altogether, 16 quantitative features, a single qualitative character and two derived ratios were scored on 33 specimens. The libraries NumPy (Oliphant 2015) and Pandas (McKinney 2010) were utilized to load and process the morphometric matrix in Python ver. 3.6.6. The similarity of specimens was measured by Gower's coefficient *GOW* (Gower 1971):

$$GOW_{ij} = \frac{\sum_{k=1}^{n} w_{ijk} s_{ijk}}{\sum_{k=1}^{n} w_{ijk}},$$

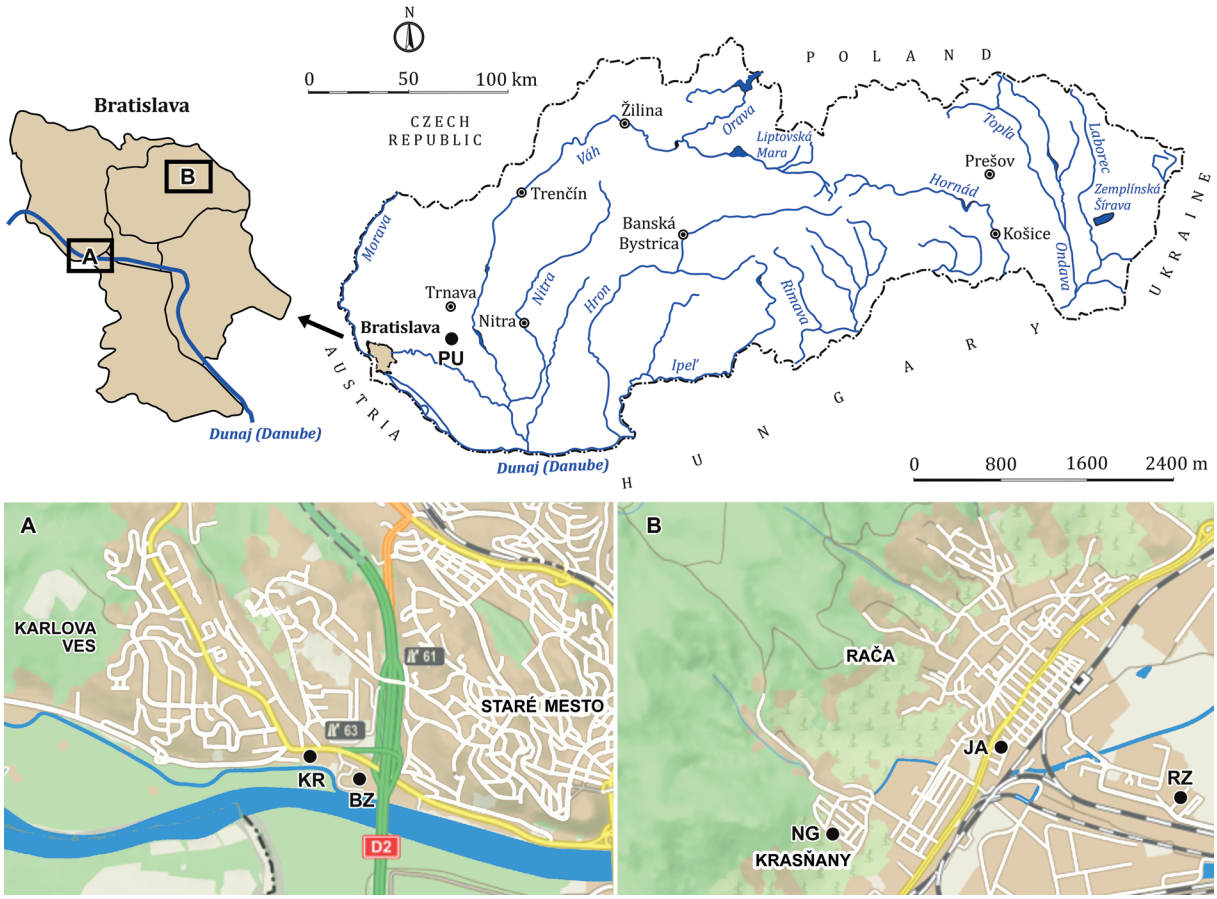

Fig. 1. Map of Slovakia showing the localization of six collection sites (marked by black dots). A schematized outline of Bratislava City is depicted left of the map of Slovakia. Rectangles A and B indicate the two Bratislava study areas, whose details are shown in panels (A) and (B) under the map of Slovakia. For locality codes and further details, see Table 1.

Table 1. Characterization of collection sites of earthworm species examined for the presence of astome ciliates. For localization of localities, see Fig. 1.

Collection date	Collection site	Locality code	GPS coordinates	Host species
6 Jun. 2017	Agricultural, brown soil from a garden, Šúrska ulica street, Rendez, Bratislava	RZ	48°11′57.6″ N, 17°10′25.0″ E	*Lumbricus terrestris* Linnaeus, 1758
3 Oct. 2017	Floodplain soil from a riparian, willow-poplar forest near the Karlova Ves branch of the Danube river, Bratislava	KR	48°08′47.5″ N, 17°04′08.0″ E	*Lumbricus terrestris* Linnaeus, 1758
19 May 2018	Decomposing plant material from a compost heap in the Botanical Garden, Karlova Ves, Bratislava	BZ	48°08′43.5″ N, 17°04′21.1″ E	*Eisenia fetida* (Savigny, 1826)
28 Jun. 2018	Decomposing plant material and humous soil from a garden compost heap, Jakubská ulica street, Rača, Bratislava	JA-1	48°12′10.9″ N, 17°09′05.7″ E	*Eisenia fetida* (Savigny, 1826)
28 Jun. 2018	Loamy soil with fallen needles in the surroundings of a garden wall, Jakubská ulica street, Rača, Bratislava	JA-2	48°12′12.2″ N, 17°09′03.1″ E	*Lumbricus terrestris* Linnaeus, 1758
30 Jun. 2018	Humous soil with high content of decomposing plant material from a garden at the foothill of the Malé Karpaty Mts., Na Grunte street, Krasňany, Bratislava	NG	48°11′44.4″ N, 17°07′47.5″ E	*Dendrobaena veneta* (Rosa, 1886)
2 Jul. 2018	Upper 50 cm turf layer in the riparian zone of the Rašelinisko pond in the vicinity of the Pusté Úľany village, Galanta district	PU	48°13′21.9″ N 17°34′49.9″ E	*Octolasion tyrtaeum* (Savigny, 1826)

where i and j are specimens, s_{ijk} is the contribution provided by the k-th variable and w_{ijk} is 1 or 0 depending upon whether or not the comparison is valid for the k-th variable. Values of s_{ijk} for variables measured at interval and ratio scales are defined as follows:

$$s_{ijk} = 1 - \frac{|x_{ik} - x_{jk}|}{R_k},$$

where x_{ik} is the value of the k-th variable on the specimen i, x_{jk} is the value of the k-th variable on the specimen j and R_k is the range of values for the k-th variable. Values of s_{ijk} for binary qualitative variables are 1, if i and j both have the attribute k present or 0 otherwise. The weight w_{ijk} causes negative matches to be ignored. The function for computation of Gower's coefficient was obtained from https://github.com/scikit-learn/scikit-learn/pull/9555.

The similarity of specimens, as measured by Gower's index, was assessed by metric multi-dimensional scaling implemented in the scikit-learn package (Pedregosa *et al.* 2011). The SMACOF algorithm was run with 250 initializations, each run had 20 000 iterations and ε was set to 10^{-8} to declare convergence. Plotting of the ordination diagram was done with the Matplotlib module (Hunter 2007).

Molecular methods

Single cells were picked and washed in five drops of Ringer's solution (0.6%). Thoroughly washed specimens were stored in 180 µl of the cell lysis buffer CLD (Promega, Fitchburg, Wisconsin, USA) at 6°C. Genomic DNA from single cells was extracted with the ReliaPrep™ Blood gDNA Miniprep System (Promega, Fitchburg, Wisconsin, USA). The 18S rRNA gene was amplified with the universal eukaryotic primers Euk A (5'-AAC CTG GTT GAT CCT GCC AGT-3') and Euk B (5'-TGA TCC TTC TGC AGG TTC AC-3') (Medlin *et al.* 1988). Individual polymerase chain reactions (PCR) included 5 µl of the extracted template DNA, 0.4 µl of the forward and reverse primers each (10 pmol/µl) and 10 µl of the GoTaq® Long PCR Master Mix (Promega, Fitchburg, Wisconsin, USA). The final volume was adjusted to 20 µl with deionized distilled water. PCR conditions were as follows: initial hot start denaturation at 95°C for 15 min, 30 identical amplification cycles (denaturing at 95°C for 45 s, annealing at 55°C for 1 min and extension at 72°C for 2.5 min) and final extension at 72°C for 10 min. The quality of the amplified DNA was checked by electrophoresing a 1% agarose gel. PCR products were purified using calf intestinal alkaline phosphatase and exonuclease I, *E. coli* (New England Biolabs® Inc.) and sequenced on an ABI 3730 automatic sequencer (Macrogen, Amsterdam, The Netherlands).

Phylogenetic methods

Newly obtained sequences were examined in Chromas ver. 2.6.6 (Technelysium Pty Ltd.) and high-quality sequence fragments were assembled into contigs in BioEdit ver. 7.2.5 (Hall 1999). Two 18S rRNA gene alignments were generated on the GUIDANCE2 server (http://guidance.tau.ac.il/ver2/), with the MAFFT algorithm and 100 bootstrap repeats (Sela *et al.* 2015). The first alignment (referred as 'general' henceforth) included 73 taxa and served to classify the newly obtained sequences into oligohymenophorean subclasses. Representatives from all subclasses were selected to cover their diversity and sampling basically followed our previous studies (Rataj & Vďačný 2018, 2019). Members from the subclass Peniculia were used to *a posteriori* root the trees (Fokam *et al.* 2011). The second alignment (referred as 'detailed' henceforth) contained 34 sequences from the oligohymenophorean subclass Astomatia and two outgroup sequences of *Dexiotricha* Stokes, 1885 from the subclass Scuticociliatia Small, 1967. Sampling in this dataset mostly followed Fokam *et al.* (2011) and Rataj & Vďačný (2018, 2019) and served to more closely analyze the phylogenetic position of the new astome isolates. To estimate the reliability of alignments, unmasked datasets and datasets masked with a cutoff value of 0.93 were constructed.

The best evolutionary substitution models for all datasets were estimated and selected in jModelTest ver. 2.1.10 under the Akaike Information Criterion (Darriba *et al.* 2012) on the Cipres portal ver. 3.1 (http://www.phylo.org/) (Miller *et al.* 2010). Phylogenetic relationships among oligohymenophorean ciliates were reconstructed in the maximum likelihood, Bayesian and neighbor-joining framework under the GTR +Γ + I evolutionary model with parameters as estimated in jModelTest. Maximum likelihood analyses were performed in PhyML ver. 3.0 with the SPR swapping algorithm and 1000 non-parametric bootstrap replicates on the South of France bioinformatics platform (http://www.atgc-montpellier.fr/phyml/) (Guindon *et al.* 2010). Bayesian inferences were conducted on the Cipres portal ver. 3.1 in the program MrBayes on XSEDE ver. 3.2.6 (Ronquist *et al.* 2012). Prior parameters of the GTR +Γ + I evolutionary model were implemented with the 'lset' and 'prset' commands in the MrBayes command block. Two runs, each having four (one cold and three heated) simultaneous Markov chains, were five million generations long. The sampling frequency was set to one hundred and the burn-in fraction was specified as 25%. In addition, the second set of detailed alignments was also analyzed by the neighbor-joining

algorithm in MEGA X (Kumar *et al.* 2018). All trees were computed as unrooted and were rooted *a posteriori* in FigTree ver. 1.2.3 (http://tree.bio.ed.ac.uk/software/figtree/).

Reliability of alternative tree topologies was assessed by the approximately unbiased, weighted Shimodaira-Hasegawa and weighted Kishino-Hasegawa tests (Shimodaira & Hasegawa 2001; Shimodaira 2002, 2008). Topologically unconstrained and constrained trees were constructed under the GTR +Γ + I evolutionary model, using the heuristic search, random sequence addition and the SPR swapping algorithm in the program PAUP* ver. 4.0b8 (Swofford 2003). Site-wise log likelihoods were calculated for unconstrained and constrained trees and served to calculate *p*-values for the tree topology tests in the program package CONSEL, using the commands makermt, consel and catpv (Shimodaira & Hasegawa 2001).

Average evolutionary distances among the five species of astome ciliates isolated from lumbricid earthworms, were calculated from their 18S rRNA gene alignment with the maximum composite likelihood model in MEGA X (Kumar *et al.* 2018). Standard errors of between group evolutionary distances were estimated with the bootstrap method and 1000 replicates. The rate variation among sites was modeled with a gamma distribution and the differences in the composition bias among sequences were considered in evolutionary comparisons (Tamura & Kumar 2002).

Abbreviations used in the text

AL = *Anoplophrya lumbrici*
AN = *Anoplophrya nodulata*
AU = approximately unbiased test
AV = *Anoplophrya vulgaris*
BA = bacteria
BI = Bayesian inference
CV = contractile vacuoles
DV = *Dendrobaena veneta*
EF = *Eisenia fetida*
EN = envelope of macronucleus
F = fibers
G = granules
H = fibrillar hook
LT = *Lumbricus terrestris*
MA = macronucleus
MI = micronucleus
ML = maximum likelihood
MT = *Metaradiophrya lumbrici*
MV = *Metaradiophrya varians*
NJ = neighbor-joining
OT = *Octolasion tyrtaeum*
OTU = operational taxonomic unit
SC = somatic cilia
SK = somatic kineties
VE = vesicules
WKH = weighted Kishino-Hasegawa test
WSH = weighted Shimodaira-Hasegawa test

Table 2. Occurrence of astome ciliates in earthworm species examined during the course of this study.

Collection site[a]	Host species	Endosymbiont species[b]				
		MT	MV	AL	AV	AN
RZ	*Lumbricus terrestris*	+	–	+	–	–
KR	*Lumbricus terrestris*	+	–	+	–	–
BZ	*Eisenia fetida*	–	+	–	+	–
JA-1	*Eisenia fetida*	–	+	–	+	–
JA-2	*Lumbricus terrestris*	+	–	+	–	–
NG	*Dendrobaena veneta*	–	–	–	+	–
PU	*Octolasion tyrtaeum*	–	–	–	–	+

[a] For locality codes, see Table 1.
[b] For species' abbreviations, see Material and methods.

Results

Diversity of astome ciliates in the gastrointestinal tract of lumbricid earthworms

In total, 300 earthworms were investigated for astome ciliates: 150 specimens of *Lumbricus terrestris*, 120 individuals of *Eisenia fetida*, 25 exemplars of *Dendrobaena veneta* and five specimens of *Octolasion tyrtaeum*. Five species of endosymbiotic astome ciliates were isolated from their gastrointestinal tract: *Metaradiophrya lumbrici*, *M. varians*, *Anoplophrya lumbrici*, *A. vulgaris* and *A.* cf. *nodulata* (Table 2).

Occurrence and abundance of astome ciliates were highly variable. Immature earthworms typically did not contain any ciliates, only bacterial clumps and sometimes nematodes. About one half of mature earthworms exhibiting a clitellum was inhabited by 10 to 50 ciliates per oligochaete. Sometimes, a mass occurrence of *M. lumbrici* was recorded in earthworms longer than 15 cm. Endosymbionts were typically found in the middle part of the gastrointestinal tract.

Descriptions of five astome ciliates isolated from lumbricid earthworms

Phylum Ciliophora Doflein, 1901
Subphylum Intramacronucleata Lynn, 1996
Class Oligohymenophorea de Puytorac *et al.*, 1974
Subclass Astomatia Schewiakoff, 1896
Order Astomatida Schewiakoff, 1896
Family Radiophryidae de Puytorac *et al.*, 1972

Genus *Metaradiophrya* Jankowski, 2007

Metaradiophrya lumbrici (Dujardin, 1841)
Figs 2, 3, 4, 5

Description

The body size is about 105–230 × 55–130 μm, with an average of 170 × 100 μm. The shape is ovate to elliptical with an anterior body end rounded and posterior end broadly rounded to truncate. The cell is distinctly dorsoventrally flattened (Figs 2A, F, 3B, F–M, 4A–B, E–F). On the ventral side, about 10 μm away from the anterior body end, there is a conspicuous fibrillar hook composed of two unequally long arms. The longer arm is 25–35 μm long, flat and completely situated underneath the cell surface. The shorter arm is 8–13 μm long, usually appears slightly more robust at the base and projects from the cell

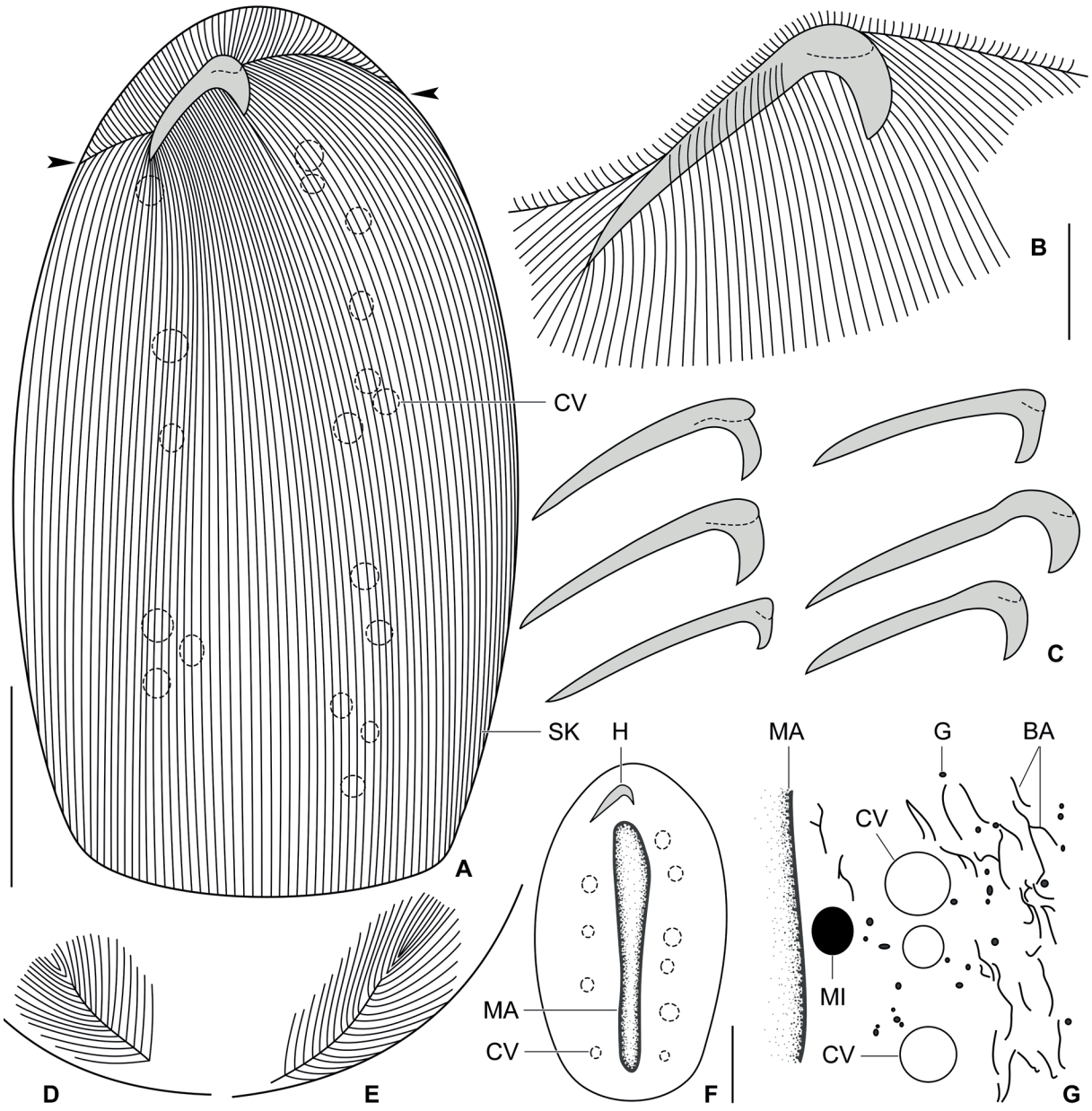

Fig. 2. *Metaradiophrya lumbrici* (Dujardin, 1841), Slovak specimens *in vivo*. **A**. Semi-schematic diagram of the ventral side, showing the fibrillar hook as well as the contractile vacuole and the somatic ciliary pattern. Arrowheads mark the subapical suture extending from the right body margin over the hook towards the left body margin. **B**. Detail of the anterior body portion, showing the fibrillar hook and its associated fibers. There are on average 6 (5–7) fibers attached to the upper right side of the longer arm, on average 33 (30–37) fibers to the ventral side of the longer arm and on average 11 (8–13) fibers to the left side of the shorter arm. **C**. Shape variants of fibrillar hooks. The hook is composed of two unequally long arms: the longer arm is flat and 25–35 µm long, while the shorter arm appears slightly more robust at the base and is 8–13 µm long. **D–E**. Lateral somatic kineties form a right and a left subterminal suture in the posterior body region. **F**. Ventral view, showing the general body organization. **G**. The cytoplasm contains innumerable granules being ca 0.4 µm across and rod-like bacteria being about 3–15 µm long. Scale bars: A, F = 50 µm; B = 10 µm.

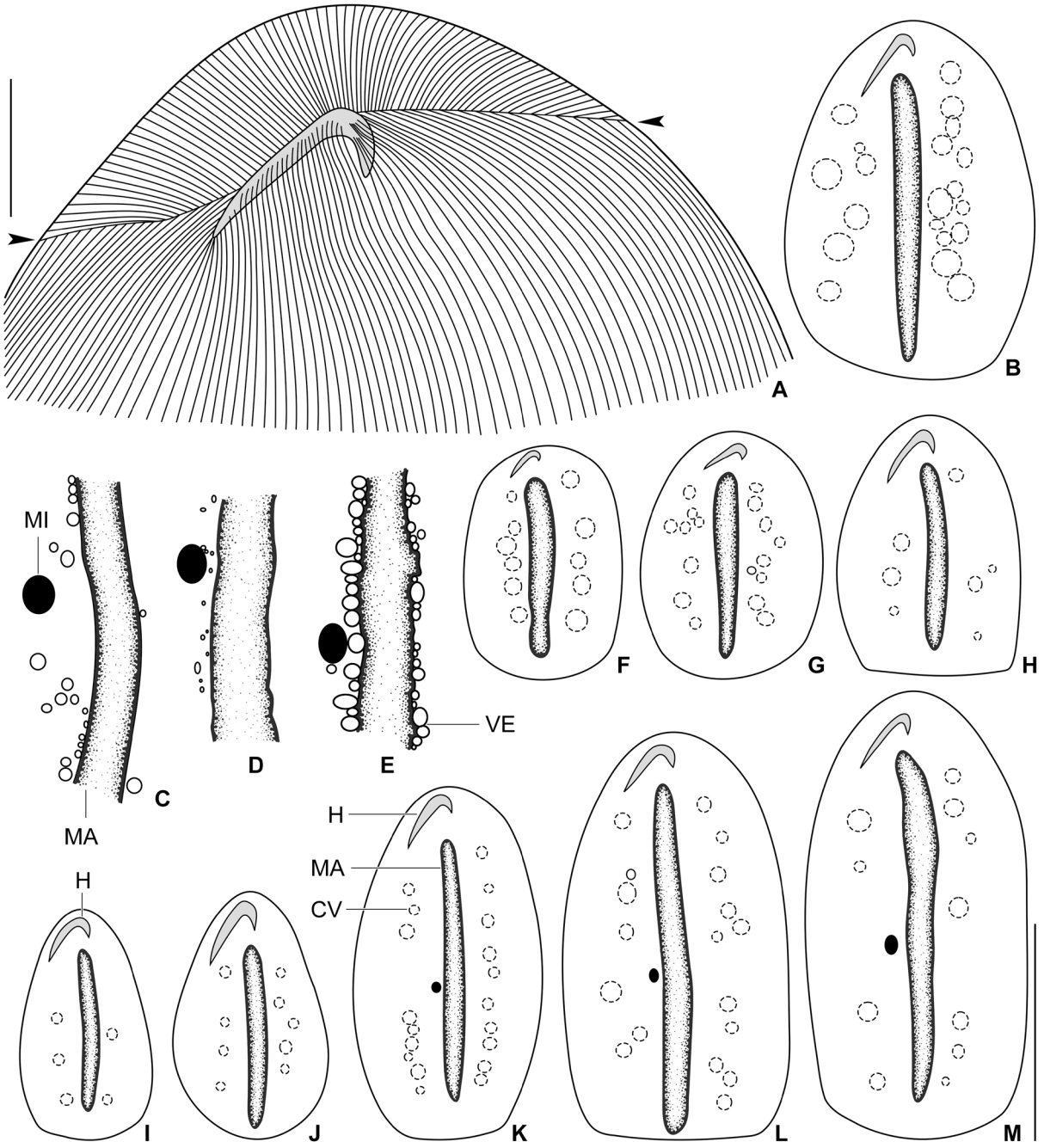

Fig. 3. *Metaradiophrya lumbrici* (Dujardin, 1841), Slovak specimens *in vivo*. **A**. Detail of the anterior body portion, showing the fibrillar hook and its associated fibers. There are on average 6 (5–7) fibers attached to the upper right side of the longer arm, on average 33 (30–37) fibers to the ventral side of the longer arm and on average 11 (8–13) fibers to the left side of the shorter arm. Arrowheads mark the subapical suture extending from the right body margin over the fibrillar hook towards the left body margin. **B, F–M**. Variability of body shape and size as well as of the contractile vacuole and nuclear apparatus. Drawn to scale. **C–E**. The macronucleus is rod-like and its surface is smooth or with some indistinct irregularities. However, many small vesicules appear in its vicinity in dying cells. The micronucleus is elliptical and typically situated close to the mid-portion of the macronucleus. Scale bars: A = 20 μm; B, F–M = 100 μm.

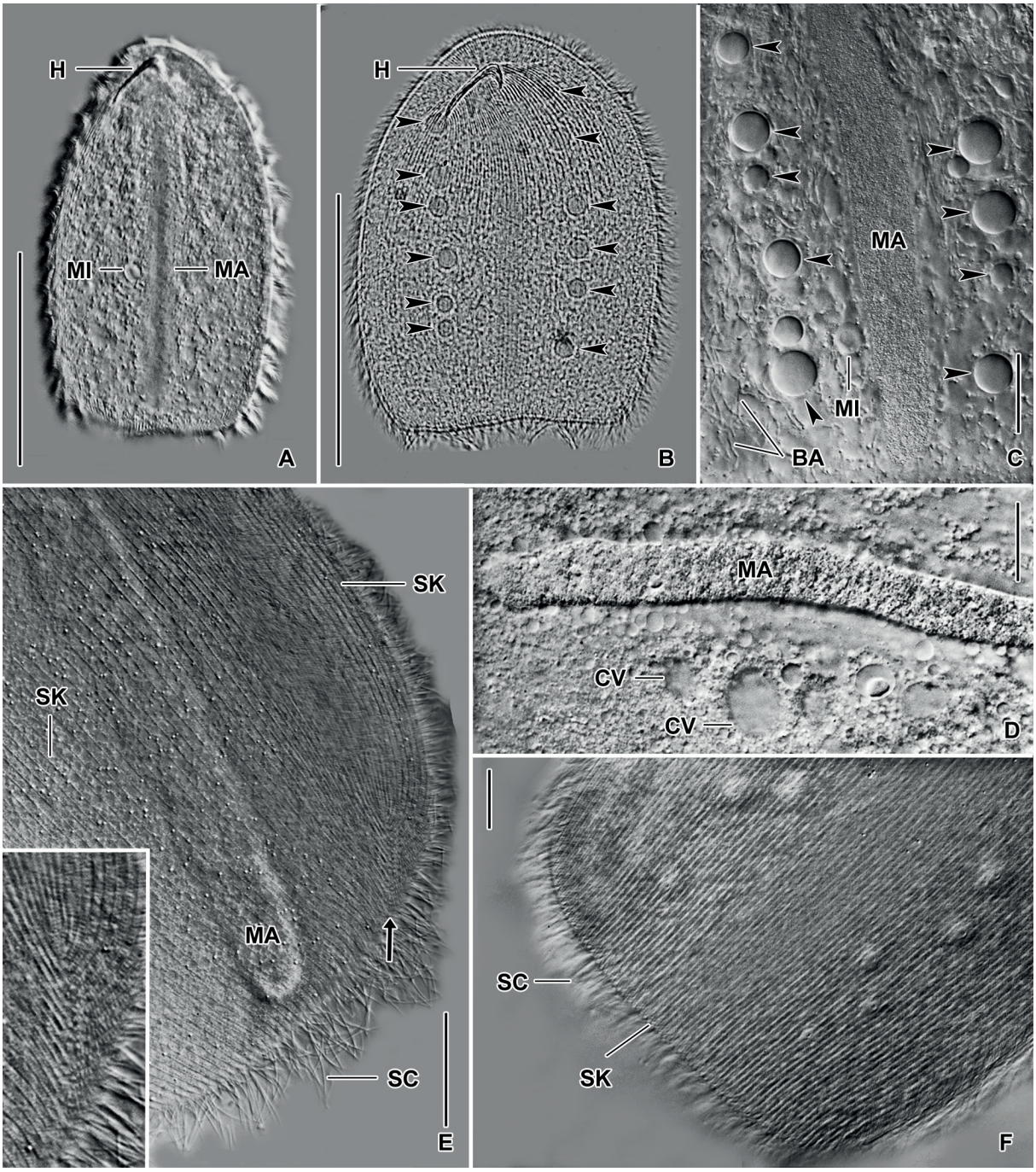

Fig. 4. *Metaradiophrya lumbrici* (Dujardin, 1841), Slovak specimens *in vivo*. **A–B**. Ventral view of representative specimens, showing the typical body shape, localization of the fibrillar hook, the long rod-like macronucleus and two staggered rows of contractile vacuoles (arrowheads). **C–D**. Detail, showing the long rod-like macronucleus, a single micronucleus, contractile vacuoles and cytoplasmic bacteria. The central region of the micronucleus appears homogenous and brighter than its margin in the differential interference optics and might represent a central nucleolus. **E–F**. Somatic ciliature is holotrichous and composed of very densely ciliated meridional kineties. In the posterior body region, lateral somatic kineties form a right and a left subterminal suture (arrow in E), whose detail is shown in the left inset. Scale bars: A–B = 100 μm; C–D = 10 μm; E–F = 20 μm.

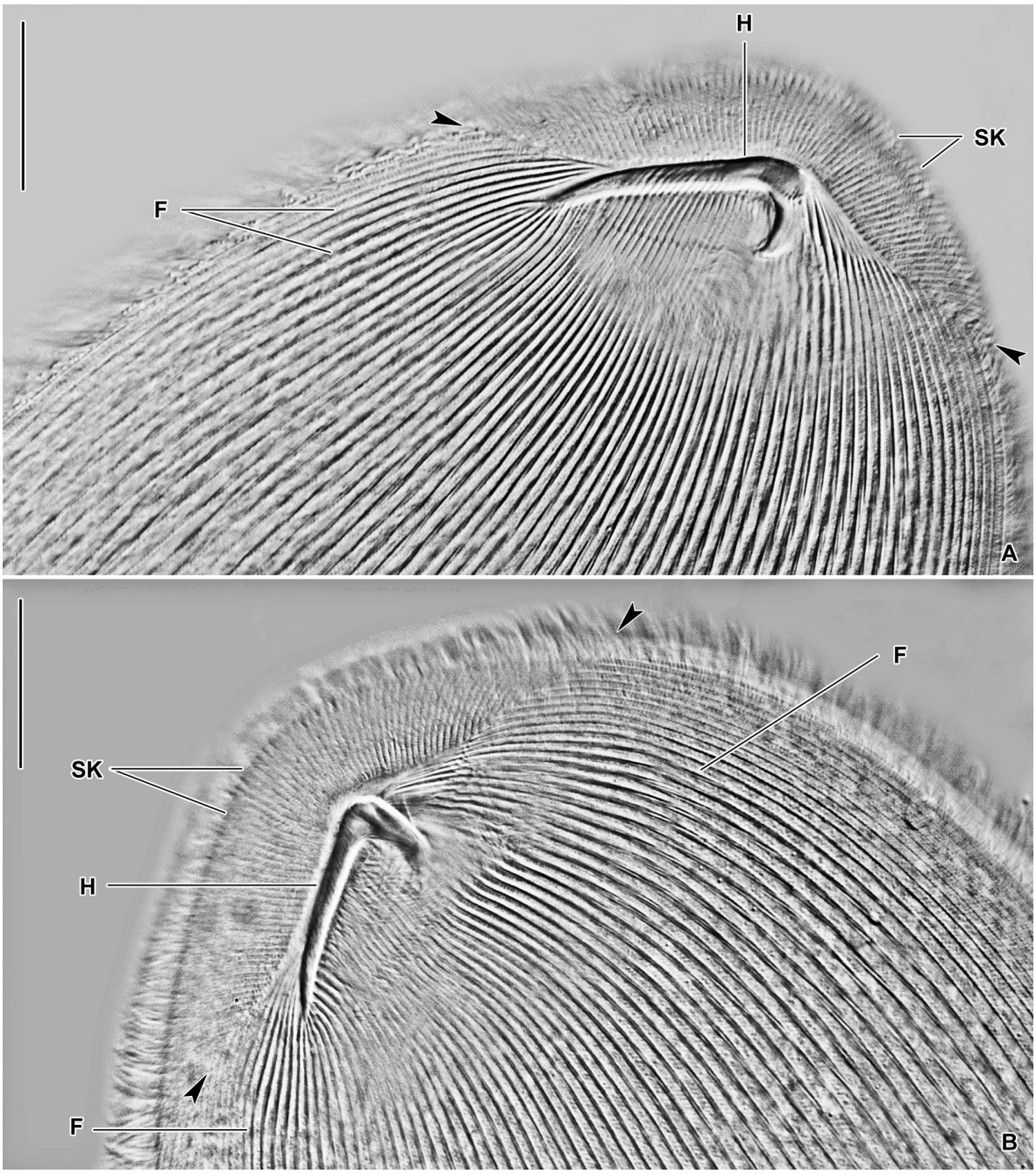

Fig. 5. A–B. *Metaradiophrya lumbrici* (Dujardin, 1841), Slovak specimens *in vivo*. Details of the anterior body portion, showing the fibrillar hook and its associated fibers. There are on average 6 (5–7) fibers attached to the upper right side of the longer arm, on average 33 (30–37) fibers to the ventral side of the longer arm and on average 11 (8–13) fibers to the left side of the shorter arm. Arrowheads mark the subapical suture extending from the right body margin over the fibrillar hook towards the left body margin. The somatic kineties above the suture run towards the anterior body end where they curve onto the dorsal body side to meridionally extend over its surface towards the posterior body end. On the other hand, the somatic kineties below the suture run meridionally over the ventral side towards the posterior body end. The ventral somatic kineties are lined with fibers attached to the fibrillar hook. Scale bars: 20 μm.

in lateral view. A set of very distinct fibers is associated with the hook: on average 6 (5–7) fibers are attached to the upper right side of the longer arm, on average 33 (30–37) fibers to the ventral side of the longer arm and on average 11 (8–13) fibers to the left side of the shorter arm (Figs 2A–C, 3A, 5).

The nuclear apparatus is composed of a macronucleus and a micronucleus. The macronucleus is rod-like with both ends rounded. It begins about 27 μm away from the anterior body margin and ends about 12 μm above the posterior body margin. Its length spans a range from approximately 85 to 200 μm and its width ranges from 8 to 18 μm, averaging at 13 μm. The macronuclear surface is smooth and without any irregularities, however, small vesicules appear in its vicinity in dying cells. The micronucleus is typically situated close to the mid-portion of the macronucleus. The shape of micronucleus is circular to elliptical and its diameter is approximately 7 μm. The central region of micronucleus appears homogenous and brighter than its margin in the differential interference optics and might represent a central nucleolus (Figs 2F–G, 3B–M, 4A, C–D).

There are invariably two staggered rows of contractile vacuoles, extending right and left of the macronucleus. Their number ranges from 3 to 12 with an average of 6 vacuoles in the right row and from 3 to 11 with an average of 6 vacuoles in the left row (Figs 2A, F–G, 3B, F–M, 4B–D). The cytoplasm is colorless and contains innumerable granules being ca 0.4 μm across and rod-like bacteria being about 3–15 μm long (Figs 2G, 4C–D). The cortex is rigid and without any specific granules (Fig. 5). Swims moderately fast by rotation about the main body axis.

Somatic ciliature is holotrichous and composed of very densely ciliated and narrowly spaced kineties. The ventral ciliature is interrupted by a subapical suture that extends from the right body margin over the fibrillar hook towards the left body margin. Somatic kineties above the suture run towards the anterior body end where they curve onto the dorsal body side to meridionally extend over its surface towards the posterior body end. Somatic kineties below the suture run meridionally over the ventral side towards the posterior body end (Figs 2A–B, 3A, 4E–F, 5). The number of kineties on each body side ranges from 60 to 78. Lateral kineties form a right and a left subterminal suture in the posterior body region (Figs 2D–E, 4E).

Occurrence

Metaradiophrya lumbrici was detected exclusively in a group of anecic earthworms, namely, in *L. terrestris* at three localities: in gardens in the Šúrska ulica street in Rendez and in the Jakubská ulica street in Rača as well as in floodplain soils in a riparian, willow-poplar forest near the Karlova Ves branch of the Danube River (Table 2). Ciliates were typically isolated from the middle part of the gastrointestinal tract, although very rarely one or two specimens were recorded also slightly above and below this gut region.

Metaradiophrya varians (de Puytorac, 1954)
Figs 6, 7

Description

The body size is about 110–180 × 85–95 μm. The body shape is ovate to elliptical with an anterior body end rounded and posterior end broadly rounded to truncate. The cell is distinctly dorsoventrally flattened (Figs 6A, F–I, 7A, D). The fibrillar hook is localized about 10 μm away from the anterior body end. Its longer arm measures on average 30 μm, while its shorter arm only 11 μm. The hook appears slightly flatter than in the previous species and the thickened base of the shorter arm has been never observed. There are 5 or 6 fibers attached to the upper right side of the longer arm, on average 26 (22–29) fibers to the ventral side of the longer arm and 11 or 12 fibers to the left side of the shorter arm (Figs 6A–C, 7B).

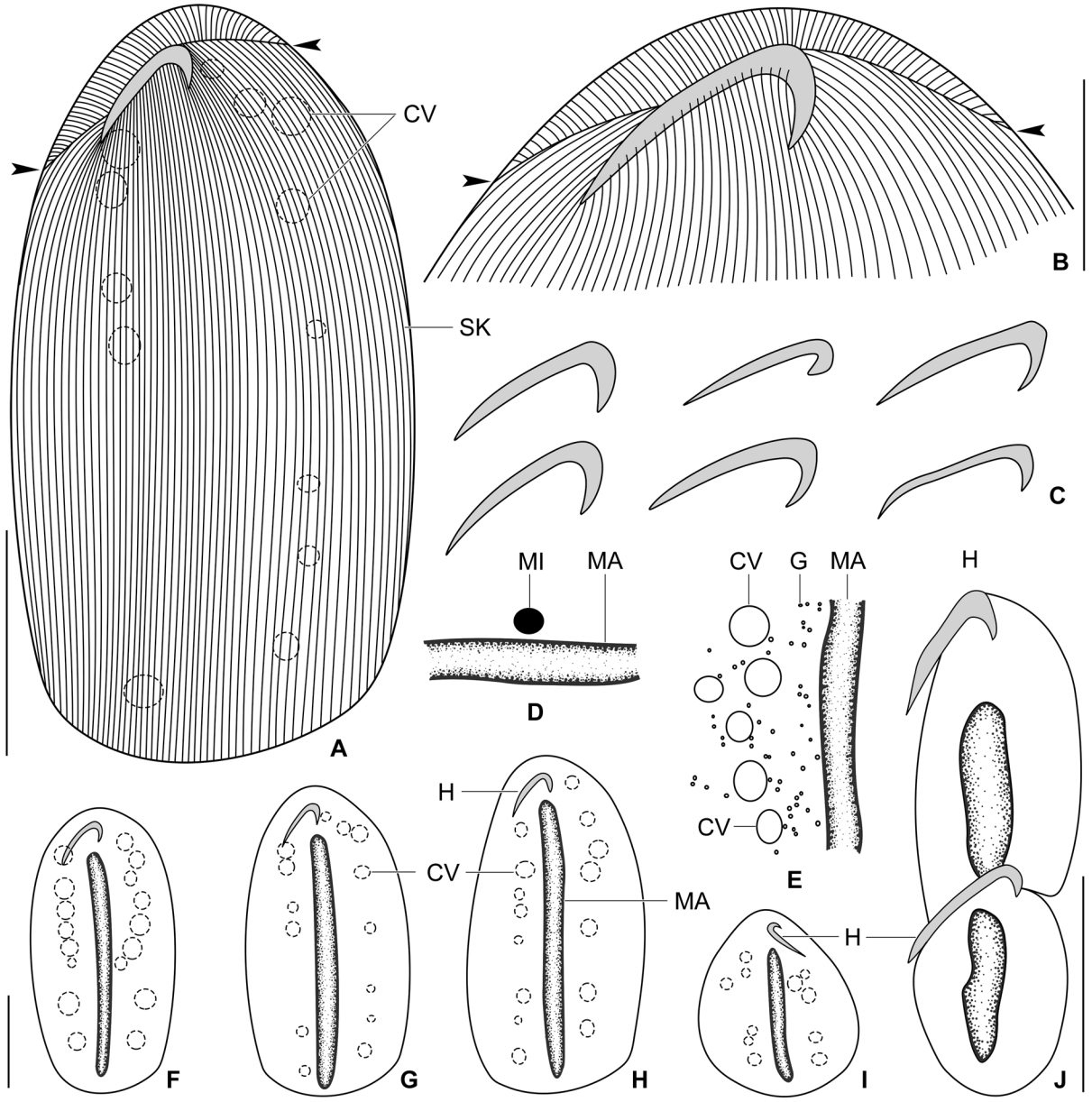

Fig. 6. *Metaradiophrya varians* (de Puytorac, 1954), Slovak specimens *in vivo*. **A**. Semi-schematic diagram of the ventral side, showing the localization of fibrillar hook, the arrangement of contractile vacuoles and the somatic ciliary pattern. Arrowheads mark the subapical suture extending from the right body margin over the fibrillar hook towards the left body margin. **B**. Detail of the anterior body portion, showing the fibrillar hook and its associated fibers. There are 5 or 6 fibers attached to the upper right side of the longer arm, on average 26 (22–29) fibers to the ventral side of the longer arm and 11 or 12 fibers to the left side of the shorter arm. **C**. Shape variants of fibrillar hooks. The longer arm of the hook measures on average 30 μm, while the shorter arm only 11 μm. **D–E**. The macronucleus is rod-like and accompanied by an elliptical micronucleus. **F–I**. Variability of body shape and size as well as of the contractile vacuole and nuclear apparatus. There are two staggered rows of contractile vacuoles arranged along the left and right side of the macronucleus. Drawn to scale. **J**. Ventral view, showing a late divider. Scale bars: A, F–J = 50 μm; B = 20 μm.

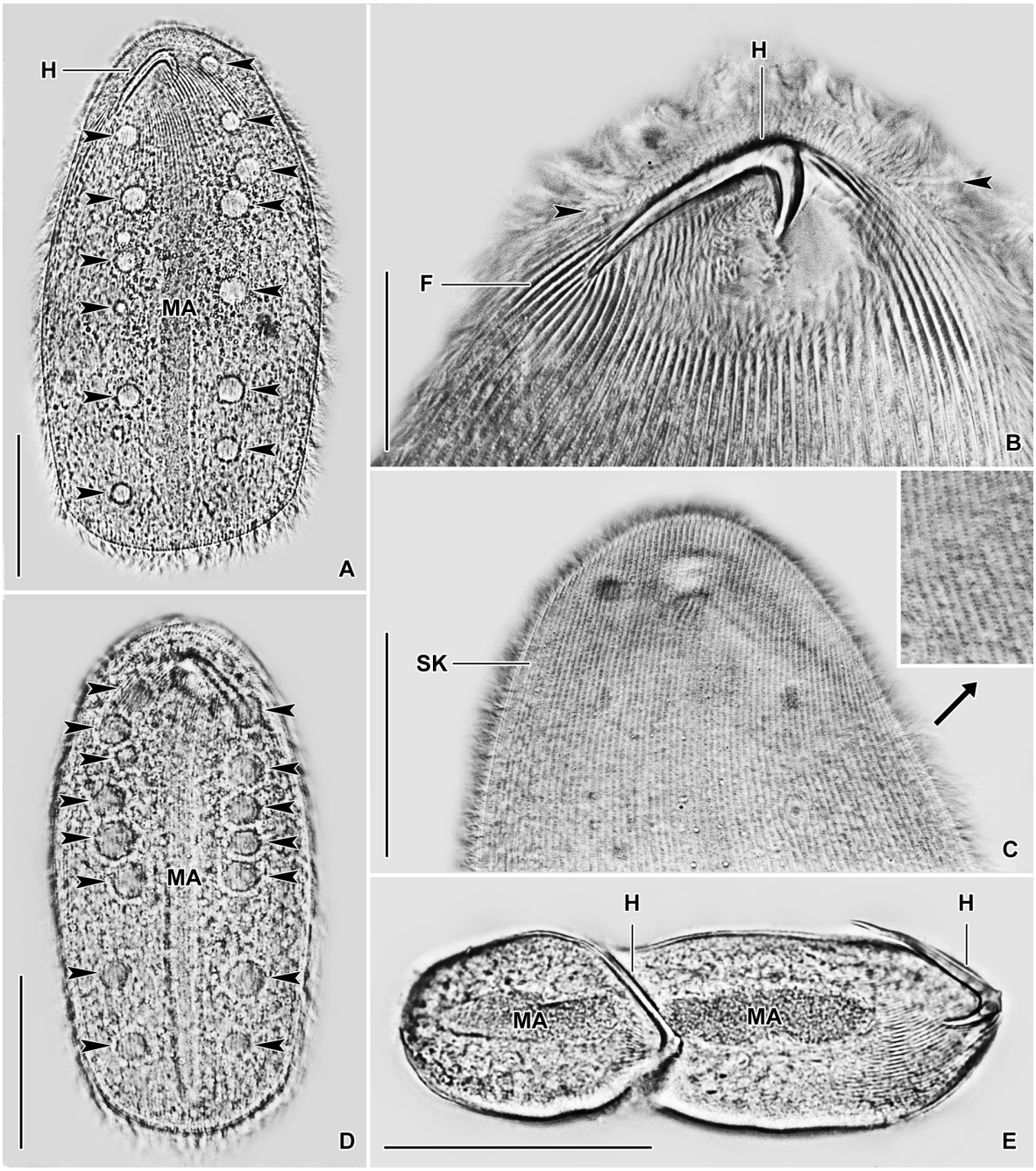

Fig. 7. *Metaradiophrya varians* (de Puytorac, 1954), Slovak specimens *in vivo*. **A, D**. Ventral view of representative specimens, showing the typical body shape, localization of the fibrillar hook, the long rod-like macronucleus and two staggered rows of contractile vacuoles (arrowheads). **B**. Detail of the anterior body portion, showing the fibrillar hook and its associated fibers. There are 5 or 6 fibers attached to the upper right side of the longer arm, on average 26 (22–29) fibers to the ventral side of the longer arm and 11 or 12 fibers to the left side of the shorter arm. Arrowheads mark the subapical suture extending from the right body margin over the fibrillar hook towards the left body margin. **C**. Dorsal view, showing the somatic kineties. The ciliary rows are narrowly arranged and are composed of very densely spaced basal bodies (left inset). **E**. Ventral view, showing a late divider. Scale bars: A, C–E = 50 µm; B = 20 µm.

The nuclear apparatus consists of a single macronucleus and a single micronucleus. The macronucleus commences on average 25 μm away from the anterior body end and terminates on average 11 μm away from the posterior body end. The size of macronucleus is about 80–140 × 10–15 μm. The macronucleus extends through cell's midline. The micronucleus reaches a diameter of 6–8 μm and is situated close to the macronucleus about in its mid-portion (Figs 6D–I, 7A, D).

There are two staggered rows of contractile vacuoles arranged along the right and left side of the macronucleus: 5–8 vacuoles in the right row and 6 or 7 vacuoles in the left row (Figs 6A, E–I, 7A, D). The cytoplasm is colorless and studded with granules about 0.5 μm across. The cortex is rigid and without granules (Fig. 7B). Swims moderately fast by rotation about the main body axis.

Somatic ciliature is holotrichous and composed of very densely ciliated and narrowly spaced kineties. The ventral ciliature is interrupted by a subapical suture extending from the right body margin over the fibrillar hook to the left body margin. Somatic kineties above the suture run towards the anterior body end where they curve onto the dorsal body side to meridionally extend over its surface towards the posterior body end. Somatic kineties below the suture run meridionally over the ventral side towards the posterior body end (Figs 6A–B, 7B–C). The number of ventral kineties ranges from 50 to 64 on the ventral side and from 53 to 64 on the dorsal side. There is a subterminal suture on the left and the right side of the body.

Occurrence

Metaradiophrya varians was solely recorded in the epigeic *E. fetida* at two comparatively distant localities, i.e., in compost heaps in the Jakubská ulica street in Rača and in the Botanical Garden of Comenius University (Fig. 1; Table 2). *Metaradiophrya varians* inhabited only the middle part of the gastrointestinal tract and there were usually ten exemplars per earthworm. Our data on occurrence of *M. varians* and *M. lumbrici* indicate that both species are specialized on different ecological groups of host oligochaetes. The ecologically different *L. terrestris* and *E. fetida* never contained the same species of *Metaradiophrya*, even when they originated from closely situated localities or when they were co-cultivated in the laboratory.

Family Anoplophryidae Cépède, 1910
Genus *Anoplophrya* Stein, 1860

Anoplophrya lumbrici (Schrank, 1803)
Figs 8, 9

Description

The body size is about 50–120 × 35–100 μm, with an average of 90 × 60 μm. The shape is broadly elliptical to elliptical with both ends rounded. The cell is distinctly dorsoventrally flattened (Figs 8A, E–I, 9A–B, D).

The nuclear apparatus consists of a single macronucleus and a single micronucleus. The macronucleus begins about 11 μm away from the anterior body end and extends through the cell's midline. The size of macronucleus varies from about 30–95 × 5–15 μm, with an average of 72 × 9 μm. The macronuclear surface is smooth to slightly irregular. In dying cells, the macronucleus diminishes in size leaving behind a conspicuous hyaline envelope. The macronucleus sometimes also fragments within the envelope in *postmortem* cells. The micronucleus is situated conspicuously far away from the macronucleus, namely, near the middle of the left body margin and always opposite to the row of contractile vacuoles. The micronucleus is globular and approximately 5 μm in diameter (Figs 8A, D–I, 9A–D).

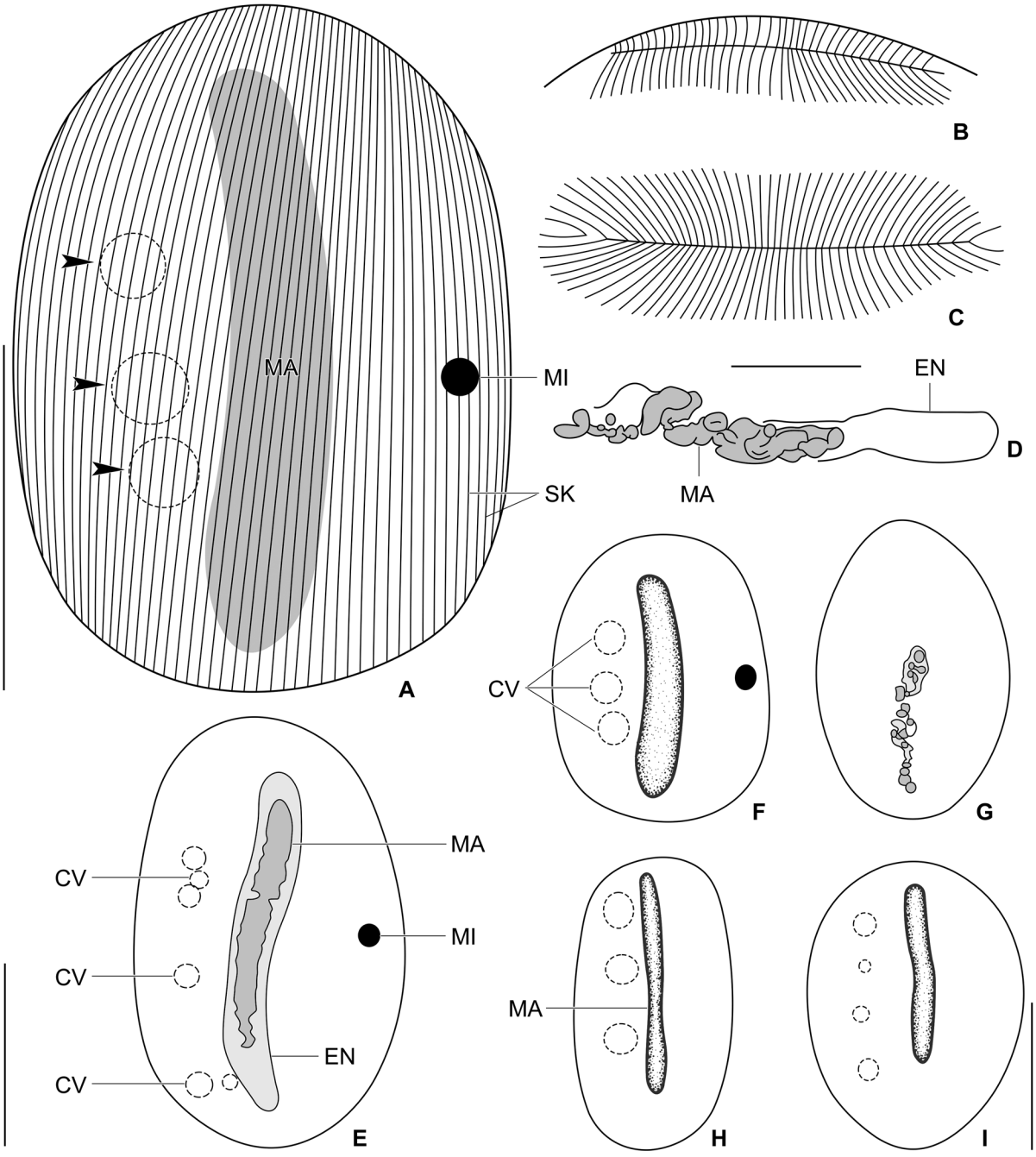

Fig. 8. *Anoplophrya lumbrici* (Schrank, 1803), Slovak specimens *in vivo*. **A**. Semi-schematic diagram of the ventral side, showing the nuclear apparatus, the arrangement of contractile vacuoles (arrowheads) and the somatic ciliary pattern. **B–C**. Details of the anterior and posterior body pole, showing the apical and the terminal suture. **D**. In dying cells, the macronucleus diminishes in size leaving behind a conspicuous hyaline envelope. The macronucleus sometimes also fragments within the envelope in *postmortem* cells. **E–I**. Variability of body shape and size as well as of the contractile vacuole and nuclear apparatus. The micronucleus is situated conspicuously far away from the macronucleus, namely, near the middle of the left body margin and always opposite to the row of contractile vacuoles. Drawn to scale. Scale bars: A, E–I = 50 μm; D = 20 μm.

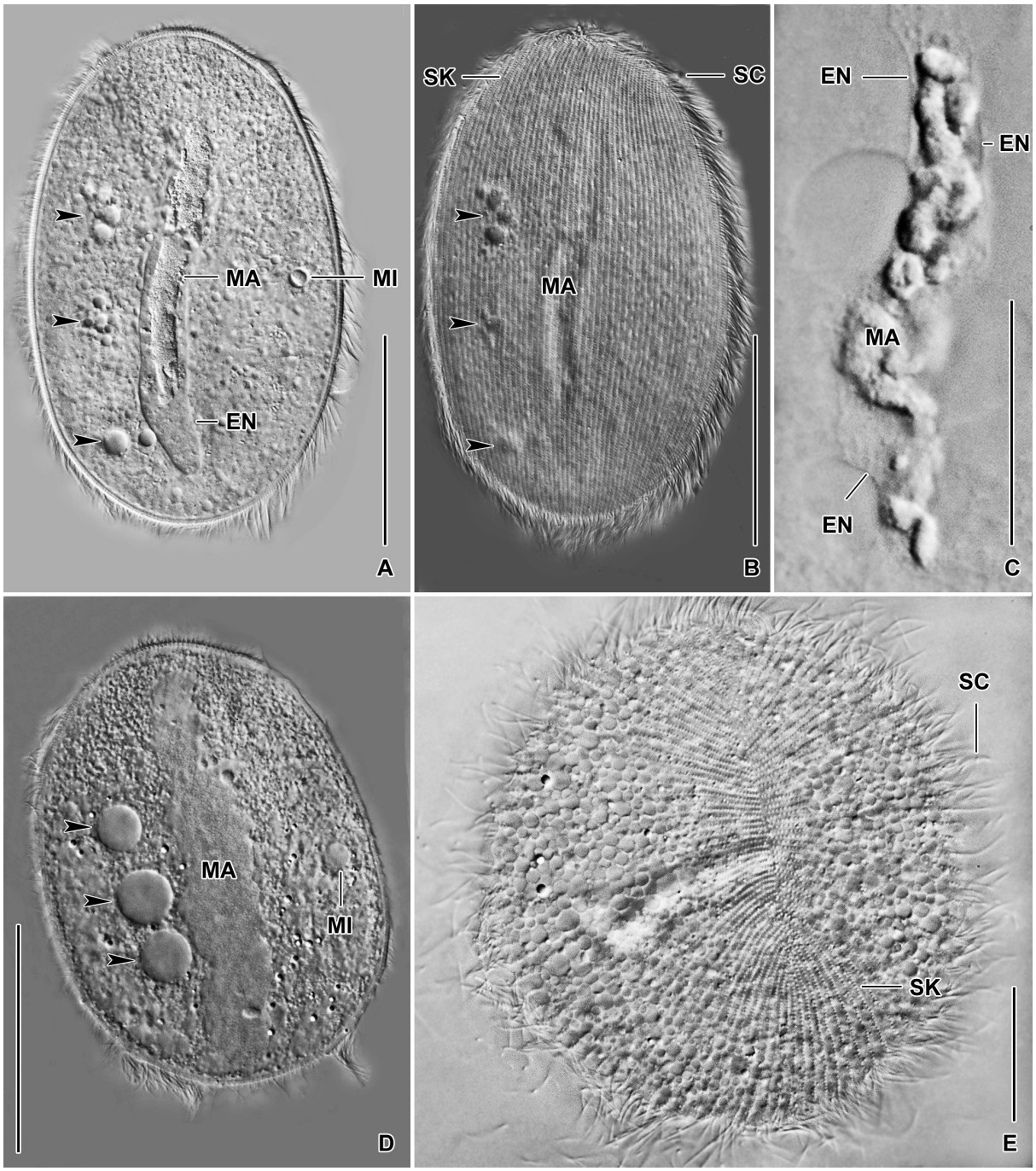

Fig. 9. *Anoplophrya lumbrici* (Schrank, 1803), Slovak specimens *in vivo*. **A, D**. Optical sections, showing the general body organization. The body is elliptical with both ends rounded. The macronucleus is rod-like and extends through the cell's midline. The micronucleus is situated conspicuously far away from the macronucleus, namely, near the middle of the left body margin and always opposite to the row of contractile vacuoles (arrowheads). **B**. Ventral view, showing the somatic ciliary pattern. Arrowheads denote the contractile vacuoles which originate by fusion of three to five vesicules. **C**. In dying cells, the macronucleus diminishes in size leaving behind a conspicuous hyaline envelope. The macronucleus sometimes also fragments within the envelope in *postmortem* cells. **E**. Frontal view, showing the apical suture. Scale bars: A–B, D = 50 μm; C, E = 20 μm.

There is only a single row of contractile vacuoles extending along the right cell margin. The number of vacuoles is three or four and their size ranges from 4 to 11 µm in diastole. A contractile vacuole originates by fusion of three to five vesicules (Figs 8A, E–F, H–I, 9A–B, D). The cytoplasm is colorless and contains innumerable granules being about 1.5 µm across. The cortex is semi-rigid and without specific granules. Swims moderately fast by rotation about the main body axis.

The somatic ciliature is holotrichous and composed of meridionally extending kineties over both cell sides. The number of ventral kineties varies from 30 to 50, averaging at 42. The number of dorsal kineties almost matches the number on the ventral side (30–51, on average 43). Somatic kineties are composed of very densely arranged basal bodies, i.e., intrakinetal distance is only 1.3 µm (Figs 8A, 9B). There is an apical and a terminal suture at the anterior and the posterior pole where individual somatic kineties begin and terminate, respectively (Figs 8B–C, 9E).

Occurrence

Anoplophrya lumbrici was recorded only in the anecic *L. terrestris* at three localities: gardens at the Šúrska ulica street in Rendez and at the Jakubská ulica street in Rača as well as in floodplain soils in a riparian, willow-poplar forest near the Karlova Ves branch of the Danube River (Table 2). Ciliates were typically isolated from the middle part of the gastrointestinal tract, although very rarely some specimens were recorded also below this gut region.

Anoplophrya vulgaris de Puytorac, 1954
Figs 10, 11A–C

Description

The body size is about 100–145 × 60–80 µm. The body shape is broadly elliptical to elliptical with both ends rounded. The cell is distinctly dorsoventrally flattened (Figs 10A, D–F, 11A–B).

The nuclear apparatus is composed of a single macronucleus and a single micronucleus. The macronucleus begins about 6 µm away from the anterior body end extends through the cell's midline into the posterior body region. The length of macronucleus varies from 80 to 110 µm and its width ranges from 9 to 18 µm. The macronuclear surface is smooth. The macronucleus diminishes in size leaving behind a conspicuous hyaline envelope in dying cells. The micronucleus is situated conspicuously far away from the macronucleus, namely, near the middle of the left body margin and opposite to the row of contractile vacuoles. The micronucleus is globular and approximately 4 µm in diameter (Figs 10A, D–F, 11A–B).

There is a single row of contractile vacuoles arranged along the right cell margin. It is composed of three or four vacuoles being 5–9 µm across during diastole (Figs 10A, D–F, 11A–B). The cytoplasm is colorless and studded with granules measuring approximately 0.5–1.0 µm in diameter. The cortex is semi-rigid and without specific granules. Swims moderately fast by rotation about the main body axis.

Somatic ciliature is holotrichous and composed of kineties meridionally extending over both cell sides. There are on average 34 (24–45) kineties on each body side. Individual kineties are very narrowly arranged and the interkinetal distance ranges from about 0.6 to 2.0 µm. Likewise, basal bodies are very narrowly spaced within kineties and the intrakinetal distance is ca 1 µm. There is an apical and a terminal suture at each cell pole where individual somatic kineties commence and terminate, respectively (Figs 10A–C, 11B–C).

Occurrence

Anoplophrya vulgaris was recorded in two species of epigeic earthworms, viz., in *E. fetida* and *D. veneta*. Ciliate 18S rRNA gene sequences originated from both hosts were identical. Host earthworms came from a compost heap in the Botanical Garden of Comenius University and at the Jakubská ulica street in Rača as well as from humous soil with a high content of decomposing plant material from a garden at the foothill of the Malé Karpaty Mts. (Table 2). Endosymbiotic ciliates typically occurred in the middle part of the gastrointestinal tract. There were usually 10 to 15 endosymbionts per host.

Anoplophrya* cf. *nodulata (Dujardin, 1841)
Figs 11D–E, 12

Description

Only five specimens were found, three were morphologically examined and two were used for molecular analyses. Therefore, the description is rather incomplete. The body size is about 100 × 50 μm. The

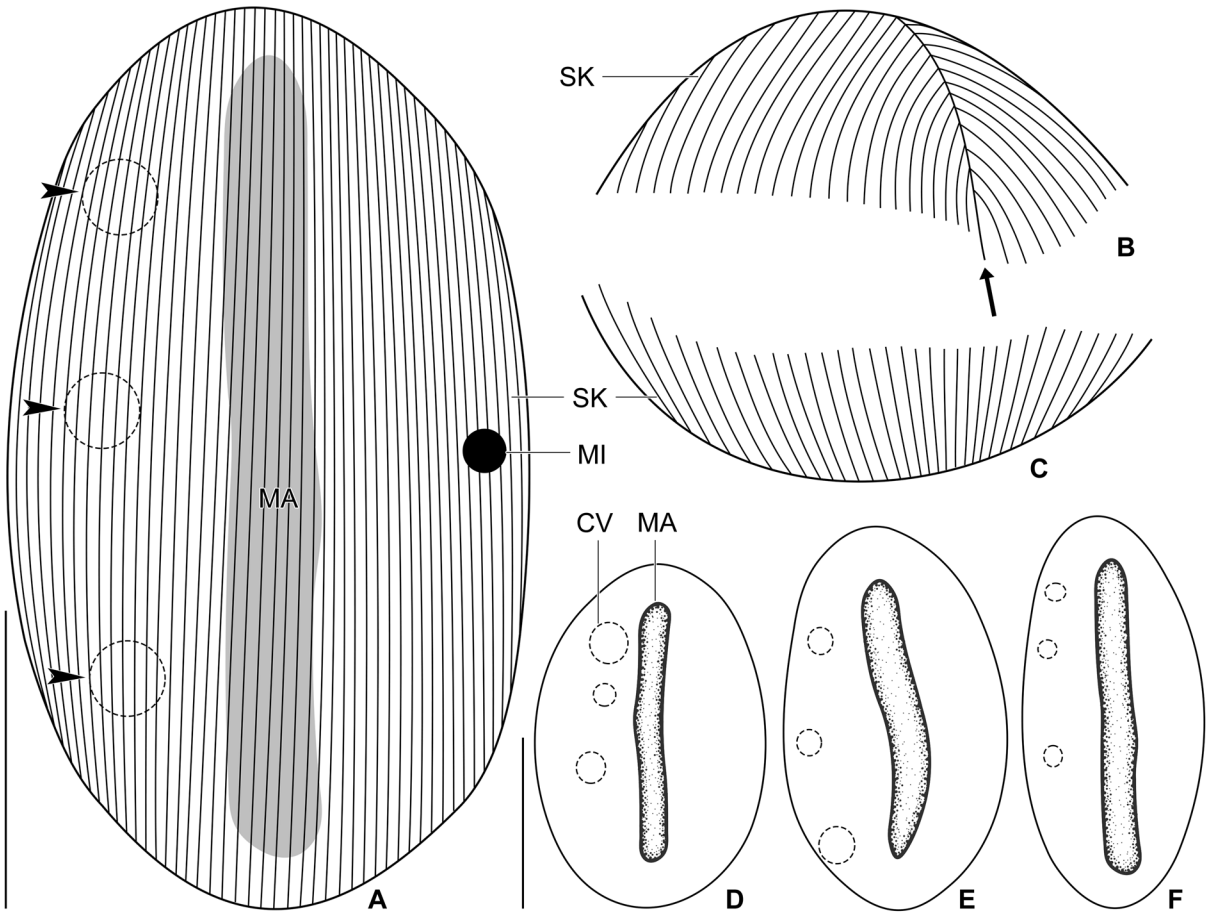

Fig. 10. *Anoplophrya vulgaris* de Puytorac, 1954, Slovak specimens *in vivo*. **A**. Semi-schematic diagram of the ventral side, showing the nuclear apparatus, the arrangement of contractile vacuoles (arrowheads) and the somatic ciliary pattern. **B–C**. Details of the anterior body pole and the posterior body region, showing the course of the somatic kineties. Arrow denotes the apical suture. **D–F**. Variability of body shape and size as well as of the contractile vacuole and nuclear apparatus. Drawn to scale. Scale bars: 50 μm.

shape is ovate to broadly fusiform with both ends rounded. The cell is distinctly dorsoventrally flattened (Figs 11D–E, 12).

The macronucleus begins about 10 μm away from the anterior body end and extends through the cell's midline. Its size is usually 75 × 13 μm. The macronuclear surface was slightly irregular. The macronucleus displays similar *postmortem* changes as in the two previous *Anoplophrya* species, i.e., it slightly diminishes in size leaving behind a hyaline envelope. The micronucleus was not observed (Figs 11D–E, 12).

There are two staggered rows of contractile vacuoles extending along the right and left side of the macronucleus: 3–6 vacuoles in the right row and 3–5 vacuoles in the left row. The average size of vacuoles ranged from 5–7 μm during diastole (Figs 11D–E, 12). The cytoplasm is colorless and filled with granules being approximately 1 μm in diameter. The cortex is semi-rigid and without specific granules. Swims moderately fast by rotation about the main body axis.

Fig. 11. *Anoplophrya vulgaris* de Puytorac, 1954 (A–C) and *Anoplophrya nodulata* (Dujardin, 1841) (D–E), Slovak specimens *in vivo*. **A–B**. Ventral views, showing the nuclear apparatus, the arrangement of contractile vacuoles (arrowheads) and the somatic ciliary pattern. Arrow marks the apical suture. **C**. Detail of the anterior body region, showing the apical suture (arrow) and the meridional ciliary rows composed of very narrowly arranged basal bodies. **D–E**. Optical sections, showing the general body organization. The body is ovate to broadly fusiform with both ends rounded. The macronucleus is rod-like with slightly irregular surface. There are two rows of contractile vacuoles (arrowheads). Scale bars: A–B, D–E = 50 μm; C = 20 μm.

Somatic ciliature is holotrichous and composed of densely ciliated meridional kineties. Due to the low number of ciliates, their number on the ventral and dorsal side could not be determined.

Occurrence

Anoplophrya nodulata was detected only in two out of five specimens of *Octolasion tyrtaeum* investigated. This endogeic earthworm originated from the upper 50 cm peat layer in the riparian zone of the Rašelinisko Pond in the vicinity of the Pusté Úľany Village in the Galanta District (Table 2). Endosymbiotic ciliates were found only in the central part of the oligochaete gastrointestinal tract. No other ciliates were recorded in the digestive system of *O. tyrtaeum*.

Multivariate morphometric analyses

Altogether, 16 quantitative features, a single qualitative character and two derived ratios were scored on 33 individuals belonging to four astome species: *M. lumbrici*, *M. varians*, *A. lumbrici* and *A. vulgaris*. Morphometric data were compiled in Table 3 and served to calculate Gower's pairwise similarities among ciliate specimens. Multidimensional scaling was performed on the pairwise Gower's coefficients, using the scikit-learn package in Python.

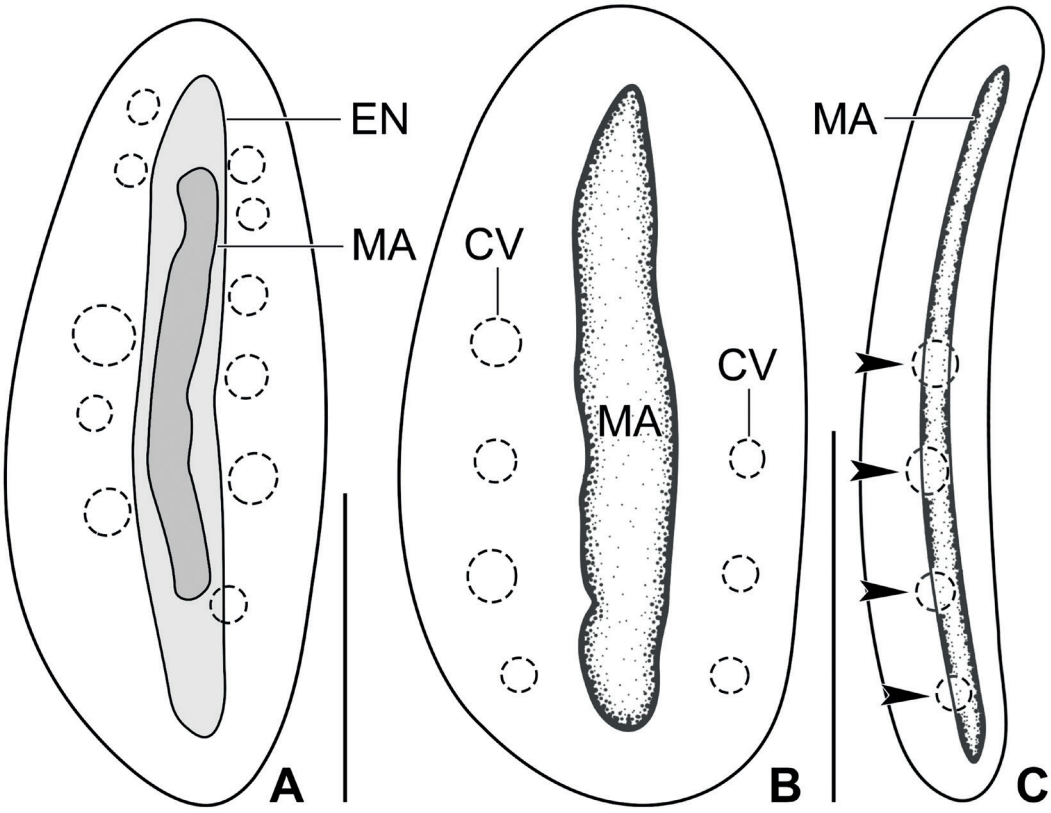

Fig. 12. *Anoplophrya nodulata* (Dujardin, 1841), Slovak specimens *in vivo*. **A**–**B**. Ventral views, showing the general body organization. The body is ovate with both ends rounded. The macronucleus is rod-like and extends through the cell's midline. In dying cells, the macronucleus diminishes in size leaving behind a conspicuous hyaline envelope. There are two rows of contractile vacuoles, extending right and left of the macronucleus. **C**. Lateral view, showing the distinctly dorsoventrally flattened body. Arrowheads denote the right row of contractile vacuoles. Scale bars: 50 μm.

Two mutually isolated groups, species of *Metaradiophrya* and *Anoplophrya*, were distinctly separated along the first and the second ordination axis (Fig. 13). However, individual species within each genus were not distinctly segregated. Specifically, two specimens of *M. varians* were intermingled with some *M. lumbrici* individuals, indicating that the intraspecific variability in most morphometric features of the latter species is so wide that *M. varians* at least partially falls within its range. Nevertheless, both species can be unequivocally distinguished by a single morphometric character, the number of fibers associated with the ventral side of the longer arm of the fibrillar hook. Specifically, there are 30–37 (on average 33) fibers in *M. lumbrici* and 22–29 (on average 26) fibers in *M. varians* (Table 3).

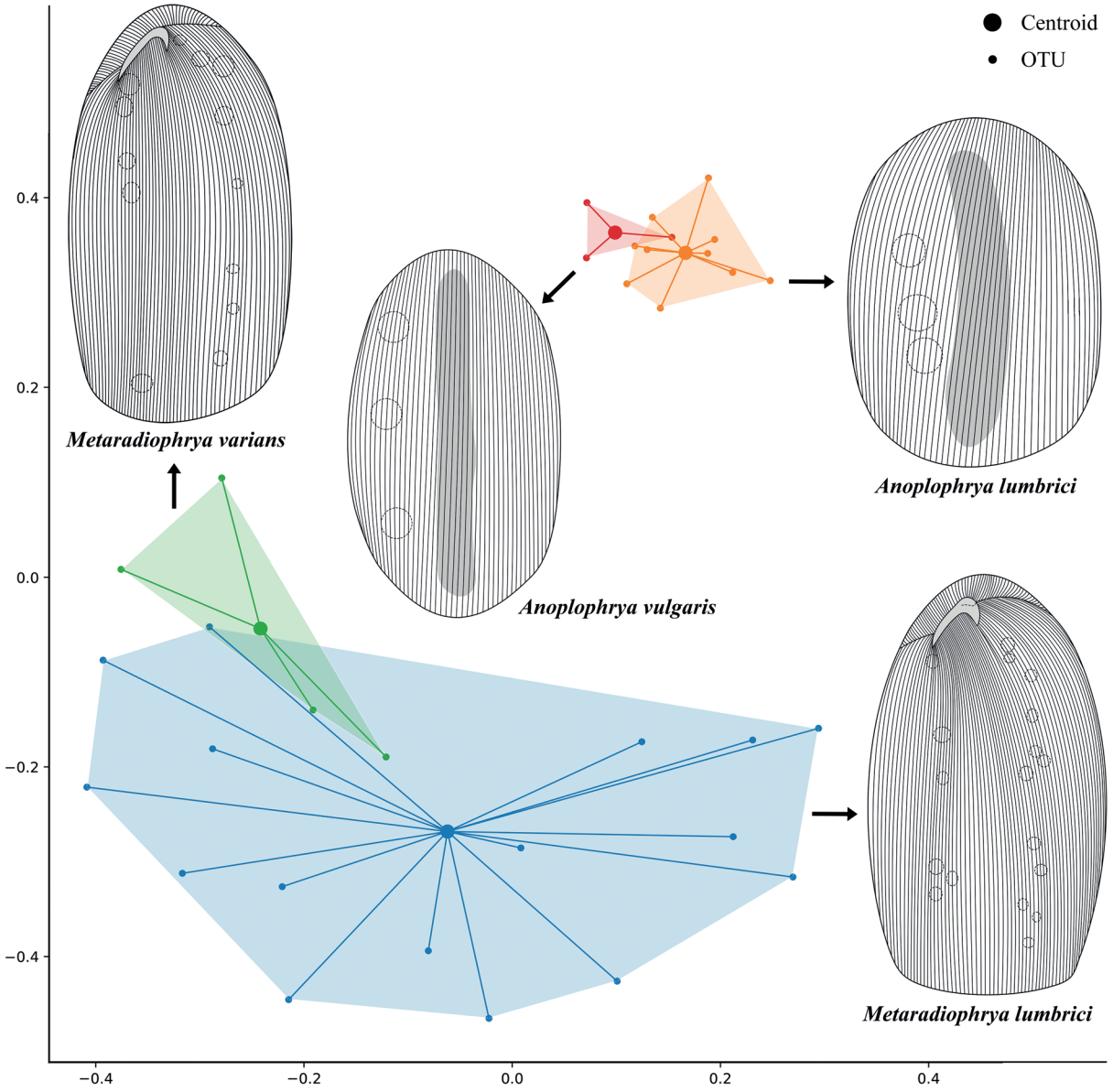

Fig. 13. Multidimensional scaling of 33 individuals based on pairwise Gower's similarities calculated from 16 quantitative features, a single qualitative character and two derived ratios.

A similar mixed pattern was revealed also for the two species of *Anoplophrya*. *Anoplophrya lumbrici* was depicted as a comparatively more variable species, somewhat overlapping with the cluster of *A. vulgaris*. The latter species, however, showed a trend of at least partial separation from *A. lumbrici* in the ordination diagram (Fig. 13). The morphometric data indicate that *A. vulgaris* is slightly larger and narrower than *A. lumbrici* (100–145 × 60–80 μm vs 50–120 × 35–100 μm), although their size ranges overlap distinctly.

Molecular characterization and phylogenetic position of ciliates isolated from lumbricid earthworms

In total, 19 new 18S rRNA gene sequences were obtained from *M. lumbrici* (eight sequences), *M. varians* (four sequences), *A. lumbrici* (two sequences), *A. vulgaris* (three sequences) and *A. nodulata* (two sequences). Their length, GC content and GenBank accession numbers are summarized in Table 4. Intraspecies sequence similarities were 100%, except for *M. lumbrici* where one out of the 1762 nucleotide positions was polymorphic. Namely, two KR-specimens (10/1 and 10/C) had guanine at the position 796 while the rest of KR-exemplars as well as all other *M. lumbrici* individuals displayed adenine there.

Genetic distances estimated under the maximum composite likelihood model showed that the evolutionary divergence between *M. lumbrici* and *M. varians* is 0.0138 ± 0.0032. A slightly larger distance was revealed between *A. lumbrici* and *A. vulgaris* (0.0168 ± 0.0037). However, evolutionary divergences between species of *Metaradiophrya* and *Anoplophrya* were more than two times greater ranging from 0.0304 to 0.0380. *Anoplophrya nodulata* was revealed as the most divergent taxon from both species of *Metaradiophrya* (0.0608–0.0627) as well as from the two other species of *Anoplophrya* (0.0717–0.0752) (Table 5).

To determine the phylogenetic position of these five ciliate species, Bayesian and maximum likelihood (ML) as well as neighbor-joining (NJ) analyses were conducted (Figs 14–15). The newly obtained sequences were classified into the paraphyletic subclass Astomatia of the class Oligohymenophorea. Paraphyly of the Astomatia was caused in that the astome *Haptophrya planariarum* (von Siebold, 1839) isolated from flatworms clustered with species of the scuticociliate genus *Dexiotricha* with full statistical support both in the Bayesian and ML analyses. All astomes isolated from annelids formed a strongly statistically supported monophylum (posterior probability 1.00, 99% ML bootstrap). Astomes from polychaetes (*Durchoniella* spp.) branched off first and were followed by a paraphyletic assemblage of astomes from endogeic oligochaetes (*Almophrya* de Puytorac et Dragesco, 1969, *Anoplophrya nodulata*, *Eudrilophrya* de Puytorac, 1969, *Metaracoelophrya* de Puytorac et Dragesco, 1969, *Njinella* Ngassam, 1983 and *Paraclausilocola* Fokam *et al.*, 2011). Lineages of astome ciliates from anecic (*M. lumbrici* and *A. lumbrici*) and epigeic (*M. varians* and *A. vulgaris*) earthworms were nested within the crown radiation of this paraphyletic cluster (Figs 14–15).

Monophylies of *M. varians*, *A. lumbrici* (including *A. marylandensis* Conklin, 1930), *A. vulgaris* and *A. nodulata* were fully statistically supported in Bayesian, ML and NJ analyses of the general and detailed alignment (Figs 14–15). However, monophyly of *M. lumbrici* was fully statistically supported only in NJ analyses (100% bootstrap) of the detailed alignment (Fig. 15) and strongly in ML analyses (91% bootstrap) of the general alignment (Fig. 14), while it was left unsupported in ML analyses of the detailed alignment and in the Bayesian inferences of both alignments. Specifically, specimens of *M. lumbrici* clustered together in Bayesian analyses of the general alignment, but with a statistically insignificant posterior probability of 0.91 (Fig. 14). On the other hand, in the Bayesian tree inferred from the detailed alignment, specimens of *M. lumbrici* were placed in a basal polytomy of a cluster containing a fully statistically supported clade of *A. lumbrici* and *A. vulgaris*. This whole assemblage, however, obtained a statistically insignificant posterior probability of 0.82 (Fig. 14) and its relevance

Table 3 (continued on next page)**.** Morphometric data on 33 specimens belonging to four astome ciliate species. V1 = body length (µm); V2 = body width (µm); V3 = body length:width ratio; V4 = distance from anterior body end to beginning of macronucleus (µm); V5 = length of macronucleus (µm); V6 = width of macronucleus (µm); V7 = length:width ratio of macronucleus; V8 = number of rows of contractile vacuoles; V9 = number of contractile vacuoles in right row; V10 = number of contractile vacuoles in left row; V11 = number of ventral somatic ciliary rows; V12 = number of dorsal somatic ciliary rows; V13 = fibrillar hook (present = 0, absent = 1); V14 = distance from anterior body end to beginning of hook (µm); V15 = length of short arm of hook (µm); V16 = length of long arm of hook (µm); V17 = number of fibres associated with upper right side of longer arm; V18 = number of fibres associated with ventral side of longer arm; V19 = number of fibres associated with left side of shorter arm.

Species	Specimen[a]	V1	V2	V3	V4	V5	V6	V7	V8	V9	V10	V11	V12	V13	V14	V15	V16	V17	V18	V19
M. lumbrici	MT JA-2 1	201	99	2.0	36	155	11	14.1	2	5	8	76	70	0	9	9	30	7	34	12
	MT JA-2 2	226	102	2.2	27	192	17	11.3	2	3	5	63	69	0	16	10	28	6	31	12
	MT JA-2 3	180	117	1.5	30	140	10	14.0	2	6	5	67	67	0	6	11	32	6	34	12
	MT JA-2 4	167	113	1.5	24	128	13	9.8	2	9	7	72	75	0	7	11	35	6	36	12
	MT JA-2 5	178	113	1.6	40	126	18	7.0	2	3	5	70	73	0	11	10	30	7	31	13
	MT JA-2 6	230	131	1.8	33	186	15	12.4	2	7	11	63	65	0	12	13	31	5	34	12
	MT JA-2 7	165	81	2.0	24	123	8	15.4	2	9	9	65	65	0	5	8	32	6	33	11
	MT JA-2 8	119	85	1.4	19	91	11	8.3	2	3	4	60	60	0	4	10	30	5	33	11
	MT JA-2 9	157	122	1.3	25	119	13	9.2	2	6	6	60	61	0	12	12	31	5	32	12
	MT JA-2 10	222	122	1.8	30	176	15	11.7	2	12	11	78	60	0	8	12	30	5	32	11
	MT JA-2 11	232	117	2.0	23	197	18	10.9	2	4	3	68	67	0	8	10	33	4	32	11
	MT JA-2 12	215	126	1.7	32	165	15	11.0	2	4	4	73	73	0	12	10	26	6	30	11
	MT KR 13	107	65	1.6	17	84	9	9.3	2	3	4	65	65	0	2	11	33	5	33	11
	MT RZ 14	142	67	2.1	27	137	13	10.8	2	4	4	67	67	0	9	8	25	6	33	11
	MT RZ 15	111	56	2.0	23	83	12	6.9	2	6	6	60	65	0	8	8	30	5	37	8
	MT RZ 16	155	85	1.8	25	113	10	11.3	2	6	4	78	78	0	13	10	29	6	34	9
M. varians	MV JA-1 1	174	87	2.0	22	138	12	11.5	2	6	6	64	64	0	8	12	32	6	27	11
	MV JA-1 2	108	93	1.2	21	78	9	8.7	2	5	6	59	59	0	6	7	27	6	29	12
	MV JA-1 3	181	96	1.9	30	141	13	10.8	2	6	6	50	53	0	10	12	30	6	27	12
	MV JA-1 4	169	85	2.0	27	132	10	13.2	2	8	7	52	55	0	12	11	31	5	22	11

Table 3 (continued).

Species	Specimen[a]	V1	V2	V3	V4	V5	V6	V7	V8	V9	V10	V11	V12	V13	V14	V15	V16	V17	V18	V19
A. lumbrici	AL JA-2 1	79	52	1.5	13	60	6	10.0	1	3		42	43	1						
	AL JA-2 2	95	70	1.4	6	83	15	5.5	1	3		45	45	1						
	AL JA-2 3	98	48	2.0	5	88	5	17.6	1	3		50	50	1						
	AL JA-2 4	95	62	1.5	7	77	12	6.4	1	3		30	30	1						
	AL JA-2 5	120	102	1.2	12	94	12	7.8	1	3		46	46	1						
	AL JA-2 6	79	69	1.1	17	48	6	8.0	1	4		42	42	1						
	AL JA-2 7	100	78	1.3	10	80	12	6.7	1	4		37	37	1						
	AL JA-2 8	96	81	1.2	11	79	5	15.8	1	3		42	51	1						
	AL JA-2 9	51	35	1.5	8	32	7	4.6	1	3		35	35	1						
	AL JA-2 10	111	70	1.6	20	80	10	8.0	1	3		50	50	1						
A. vulgaris	AV JA-1 1	99	59	1.7	8	80	9	8.9	1	3		32	32	1						
	AV JA-1 2	142	82	1.7	6	98	18	5.4	1	4		45	45	1						
	AV JA-1 3	123	60	2.1	4	110	10	11.0	1	4		24	24	1						

[a] Specimen code consists of an abbreviation of species name as specified in Table 2 and a locality code as specified in Table 1, followed by the ordinal number of the specimen investigated.

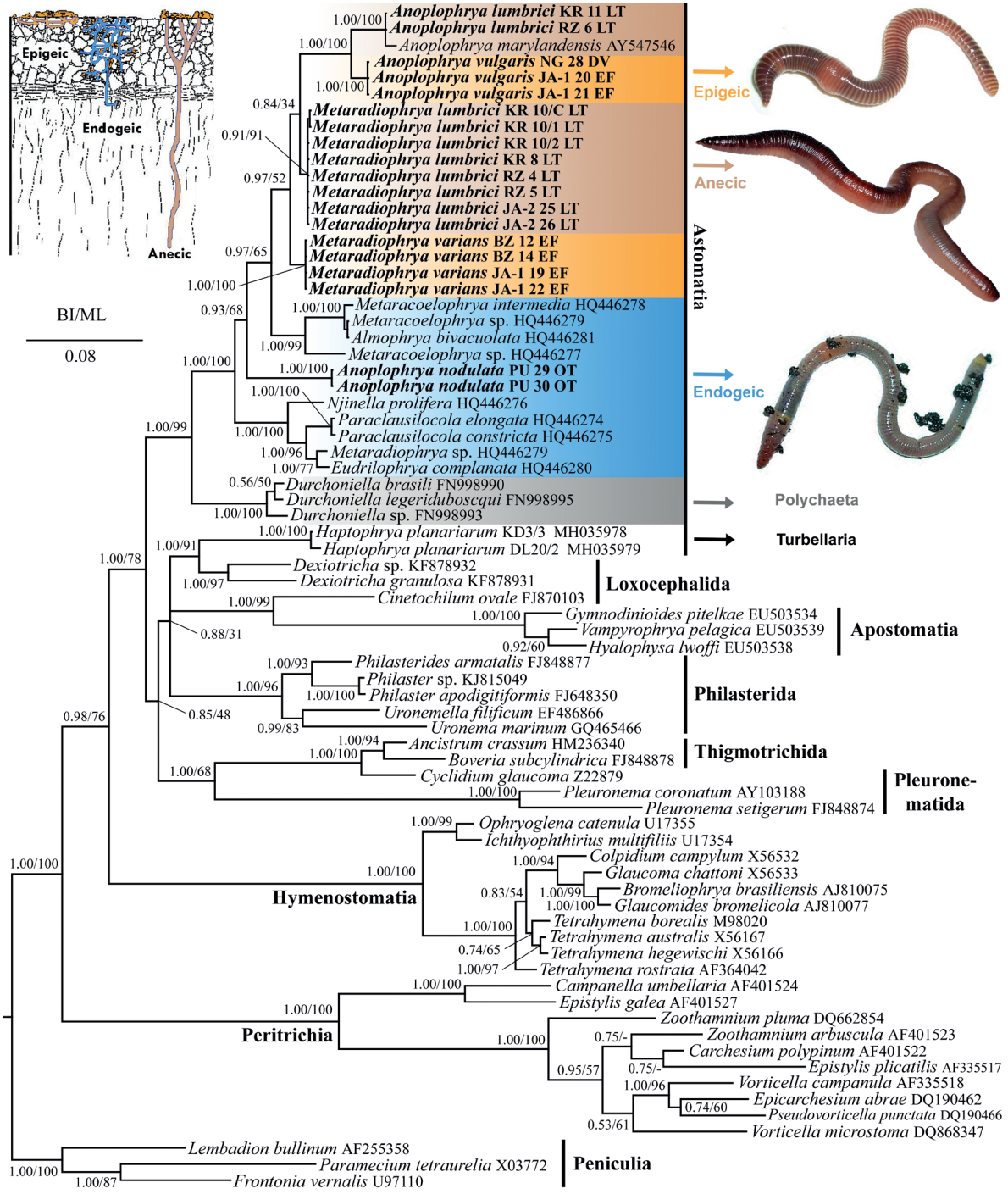

Fig. 14. Small subunit rRNA gene phylogenetic tree showing systematic positions of astome ciliates isolated from lumbricid earthworms. Posterior probabilities for Bayesian Inference (BI) and bootstrap values for Maximum Likelihood (ML) were mapped onto the 50%-majority rule Bayesian consensus tree. Dashes indicate ML bootstrap values below 50%. The phylogenetic tree suggests that the evolution of endosymbiotic astome ciliates has proceeded through a specialization to various ecological and systematic groups of their host organisms. Sequences in bold face were obtained during this study. For specimen codes and further details, see Table 4. The scale bar denotes eight substitutions per one hundred nucleotide positions.

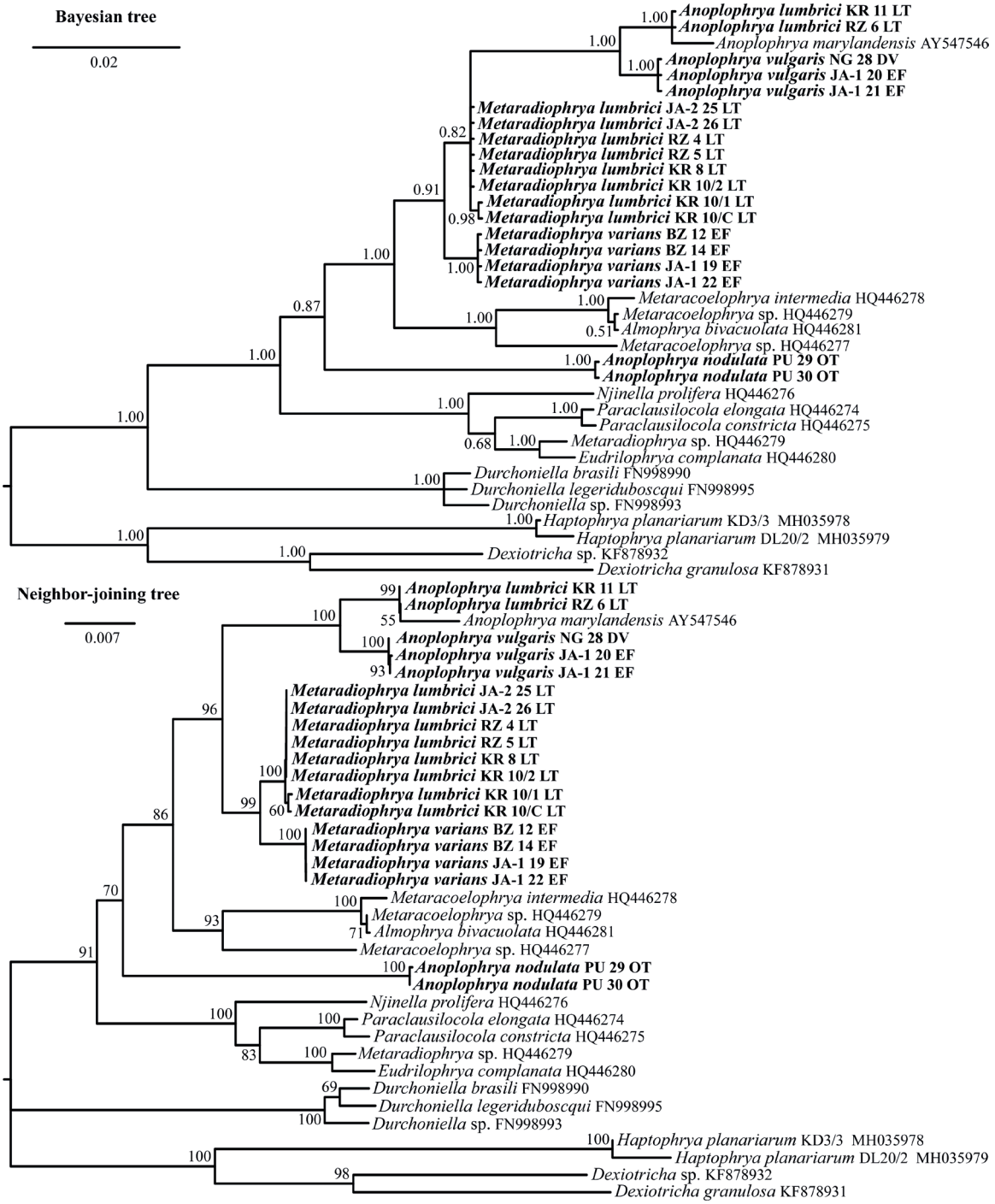

Fig. 15. Small subunit rRNA gene phylogenetic trees showing systematic positions of astome ciliates isolated from lumbricid earthworms. Posterior probabilities were mapped onto the 50%-majority rule Bayesian consensus tree (upper panel) and bootstrap values onto the 50%-majority rule neighbor-joining tree (lower panel). Sequences in bold face were obtained during this study. Note that there is a conflict between the Bayesian and the neighbor-joining tree in the position of specimens of *Metaradiophrya* Jankowski, 2007. However, according to tree topology tests, the branching pattern of the Bayesian tree is not significantly better than that of the neighbor-joining tree. The scale bar denotes fraction of substitutions.

Table 4. Characterization of new 18S rRNA gene sequences of astome ciliates obtained from lumbricid oligochaetes.

Species	Specimen[a]	Host species	Locality code[b]	Length (nt)	GC (%)	GenBank entry
Anoplophrya lumbrici	KR 11 LT	*L. terrestris*	KR	1754	43.84	MN121061
	RZ 6 LT	*L. terrestris*	RZ	1754	43.84	MN121062
Anoplophrya nodulata	PU 29 OT	*O. tyrtaeum*	PU	1758	43.86	MN121063
	PU 30 OT	*O. tyrtaeum*	PU	1758	43.86	MN121064
Anoplophrya vulgaris	JA-1 20 EF	*E. fetida*	JA-1	1750	44.57	MN121065
	JA-1 21 EF	*E. fetida*	JA-1	1750	44.57	MN121066
	NG 28 DV	*D. veneta*	NG	1750	44.57	MN121067
Metaradiophrya lumbrici	JA-2 25 LT	*L. terrestris*	JA-2	1762	44.61	MN121068
	JA-2 26 LT	*L. terrestris*	JA-2	1762	44.61	MN121069
	KR 8 LT	*L. terrestris*	KR	1762	44.61	MN121070
	KR 10/1 LT	*L. terrestris*	KR	1762	44.67	MN121071
	KR 10/2 LT	*L. terrestris*	KR	1762	44.61	MN121072
	KR 10/C LT	*L. terrestris*	KR	1762	44.67	MN121073
	RZ 4 LT	*L. terrestris*	RZ	1762	44.61	MN121074
	RZ 5 LT	*L. terrestris*	RZ	1762	44.61	MN121075
Metaradiophrya varians	BZ 12 EF	*E. fetida*	BZ	1764	44.10	MN121076
	BZ 14 EF	*E. fetida*	BZ	1764	44.10	MN121077
	JA-1 19 EF	*E. fetida*	JA-1	1764	44.10	MN121078
	JA-1 22 EF	*E. fetida*	JA-1	1764	44.10	MN121079

[a] Specimen code consists of a locality code as specified in Table 1, an isolate code and an abbreviation of host species name (see Material and methods).
[b] For locality codes, see Table 1.

should be therefore taken with great caution. Identical topology was revealed also in ML analyses of the detailed alignment (–ln L = 5056.68) (data not shown). Due to the discrepancy between the topology of the NJ tree on the one hand and the Bayesian and ML trees on the other, statistical tree topology tests were conducted. They revealed that the monophyly of *M. lumbrici* and its sister-group relationship to *M. varians* (–ln L = 5059.33) could not be rejected (Table 6). The conflict between the distance NJ tree and the Bayesian and ML trees was possibly caused by a plesiomorphic/homoplastic trap. *Meteradiophrya lumbrici* differed from *M. varians* in 25 nucleotide positions, but a comparison of 18S rRNA gene sequences of *M. lumbrici* with those of three species of *Anoplophrya* revealed that 19 out of the 25 variable nucleotide positions are either plesiomorphies or possibly homoplasies. Only six positions (36, 76, 100, 119, 120, 141) appear as molecular apomorphies of *M. lumbrici* (Fig. 16). This indicates that distance techniques might avoid the plesiomorphic/homoplastic trap when sequences of related species are highly similar (genetic distance between *M. lumbrici* and *M. varians* is only 0.0138 ± 0.0032; Table 5). On the other hand, Bayesian inference and maximum likelihood might not be resistant to the plesiomorphic/homoplastic trap when plesiomorphies/homoplasies significantly

outnumber apomorphies. Therefore, taxonomic discrepancies in phylogenetic trees need to be analyzed also using distance methods and statistical tree topology tests.

Discussion

The gastrointestinal tract of earthworms from the oligochaete family Lumbricidae is inhabited by astomes belonging to only three genera, namely, *Metaradiophrya*, *Anoplophrya* and *Maupasella* (Heidenreich 1935; Lom 1961; de Puytorac 1972). There are several dozens of species in each genus and their identification is difficult because of comparatively few diagnostic morphologic features and lack of information about intraspecific variability and host range (e.g., Cépède 1910; Heidenreich 1935; Beers 1938; Williams 1942; Lom 1961; de Puytorac 1972). Because of these problems, most records of astome ciliates from lumbricid earthworms need to be taken with caution. Moreover, our integrative approach revealed that a combination of detailed microscopic observation, molecular data as well as identity and ecological group of host organisms is indispensable for reliable identification of astomes.

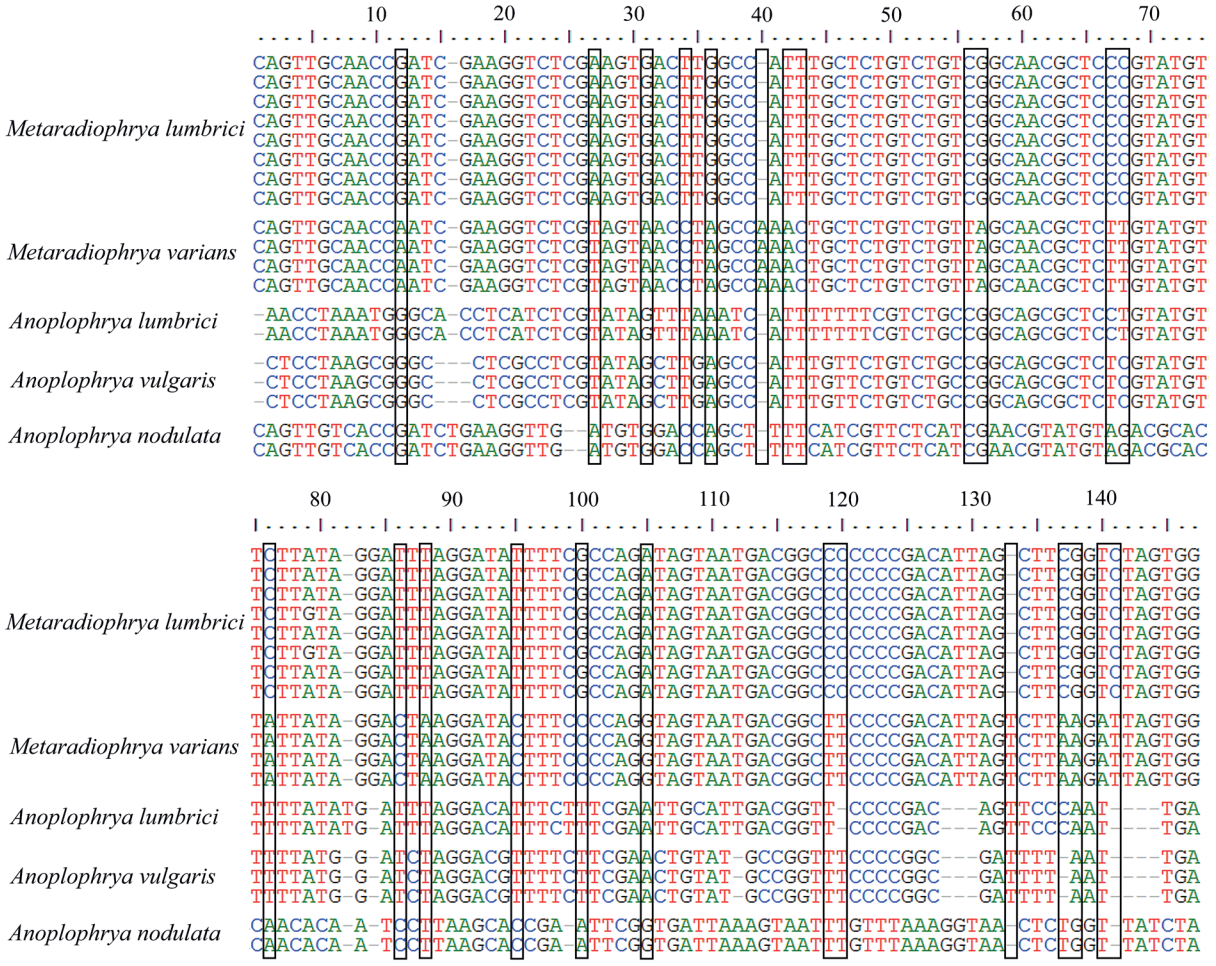

Fig. 16. Alignment of variable positions of the 18S rRNA gene of five astome ciliates isolated from the lumbricid earthworms. Boxes mark 25 nucleotide positions in which *M. lumbrici* (Dujardin, 1841) differs from *M. varians* (de Puytorac, 1954). The comparison with three outgroup species of *Anoplophrya* Stein, 1860 indicates that 19 out of the 25 variable nucleotide positions of *M. lumrici* are either plesiomorphies or possibly homoplasies.

Table 5. Average between group evolutionary distances (below diagonal) and their standard errors (above diagonal) estimated with the maximum composite likelihood method.

	1.	**2.**	**3.**	**4.**	**5.**
1. *Metaradiophrya lumbrici*	–	0.0032	0.0058	0.0056	0.0096
2. *Metaradiophrya varians*	0.0138	–	0.0066	0.0062	0.0098
3. *Anoplophrya lumbrici*	0.0318	0.0380	–	0.0037	0.0120
4. *Anoplophrya vulgaris*	0.0304	0.0352	0.0168	–	0.0113
5. *Anoplophrya nodulata*	0.0608	0.0627	0.0752	0.0717	–

Based on the integrative taxonomic approach, two species of *Metaradiophrya* were isolated from the lumbricid earthworms during the course of the present study: *M. lumbrici* and *M. varians*. The former species was detected exclusively in the group of anecic earthworms. However, Heidenreich (1935) also reported *M. lumbrici* from an ecologically different group of earthworms, namely, from the epigeic *L. rubellus* Hoffmeister, 1843 and *E. fetida* (for problems with ciliate identity, see below). Apart from *L. terrestris*, Lom (1961) recorded *M. lumbrici* also in *Dendrobaena illyrica* (Cognetti, 1906). De Puytorac (1972) extended the host spectrum of *M. lumbrici* by a further species from the family Lumbricidae, namely, *L. herculeus* (Savigny, 1826). On the other hand, Williams (1942) did not report *M. lumbrici* from the gastrointestinal tract of *L. terrestris* at all but from "*Eisenia foetidus*". *Metaradiophrya varians* has so far been reported exclusively from *E. fetida* (de Pyutorac 1954, 1972; Lom 1961; Paisán *et al.* 2009; present study). As evidenced by molecular data, we have never recorded *M. lumbrici* in *E. fetida*. All sequences of *Metaradiophrya* from this epigeic earthworm were 100% identical. According to morphometric data, they belong to *M. varians* which has a lower number of fibres associated with the ventral side of the longer arm of the hook than *M. lumbrici* (see above and de Pyutorac 1954, 1972; Lom 1961; Paisán *et al.* 2009). Therefore, we assume that Heidenreich (1935) and Williams (1942) misidentified *M. varians* as *M. lumbrici*.

According to the compendium of de Puytorac (1972), eight further species of *Metaradiophrya* were reported from earthworms of the family Lumbricidae: (1) *M. asymmetrica* (Beers, 1938) from "*Eisenia lönnbergi* (Michlsn, 1844)" [= *Eisenoides lonnbergi* (Michaelsen, 1894)]; (2) *M. bifulta* (de Puytorac, 1954) from *Helodrilus schneideri* Michaelsen, 1900; (3) *M. chlorotica* (Williams, 1942) from *Allolobophora chlorotica* (Savigny, 1826); (4) *M. falcifera* (Stein, 1861) from *L. rubellus*, *Nicodrilus caliginosus* [= *Aporrectodea caliginosa* (Savigny, 1826)] and *Octolasion lacteum* (Örley, 1881); (5) *M. gardneri* (Rees, 1961) from *Eisenia fetida*; (6) *M. gigas* de Puytorac, 1954 from *Aporrectodea savignyi* [= *Scherotheca savignyi* (Guerne & Horst, 1893)]; (7) *M. heidenreichi* (de Puytorac, 1954) from *Helodrilus schneideri*; and (8) *M. hovassei* (de Puytorac, 1954) from *Allolobophora chlorotica* and *Eisenia rosea* (Savigny, 1826).

In the course of the present study, three species of *Anoplophrya* were reported from the lumbricid earthworms: *A. lumbrici*, *A. vulgaris* and *A. nodulata*. We detected *A. lumbrici* exclusively in the anecic *L. terrestris*. Similarly, Heidenreich (1935) and de Puytorac (1972) mentioned *L. terrestris* as the host of *A. lumbrici*. Lom (1961), in addition, reported *A. lumbrici* from the epigeic earthworms *L. rubellus* and *D. subrubicunda* [= *Dendrodrilus rubidus subrubicundus* (Eisen, 1874)] in which, however, exemplars of *A. lumbrici* exhibited conspicuous morphological differences. This indicates that they might represent different species of *Anoplophrya*. Heidenreich (1935) considered *A. marylandensis* to be a junior synonym of *A. lumbrici*, which is also indicated by the present phylogenetic analyses (Figs 14–15). Sequences of *A. marylandensis* and *A. lumbrici*, originating from the same host organisms (*L. terrestris*), clustered together in our phylogenetic analyses and had a 99.3% identity. However, we cannot exclude that the difference of 0.7% in the 18S rRNA gene is sufficient to separate *A. marylandensis*

Table 6. Log likelihoods and *p*-values of the AU, WSH and WKH tests to compare different topological scenarios. Significant differences (*p*-value < 0.05) between the best unconstrained and constrained topologies in bold face.

Topology	–ln L[a]	Δ (–ln L)[b]	AU	WSH	WKH
Best scoring maximum likelihood tree (unconstrained)	5056.68	–	0.860	0.987	0.812
Monophyly of *M. lumbrici* and *M. varians*	5059.33	2.6	0.165	0.440	0.188
Monophyly of *M. lumbrici*, *M. varians* and *Metaradiophrya* sp. HQ446279	5199.22	142.5	**6e–37**	**0.000**	**0.000**
Monophyly of the genus *Metaracoelophrya*	5078.25	21.6	**0.002**	**0.016**	**0.010**

[a] Log likelihood of a phylogenetic tree.
[b] Difference between log likelihoods of constrained and best scoring (unconstrained) tree.

from *A. lumbrici*. For instance, two species of *Paraclausilocola* are morphologically clearly distinct but are only 0.3% divergent in their 18S rRNA gene sequences. Therefore, at the present state of knowledge, it might be premature to synonymize *A. marylandensis* with *A. lumbrici*. Conklin (1930) discovered *A. marylandensis* in *L. terrestris* and *Helodrilus caliginosus* [= *Aporrectodea caliginosa* (Savigny, 1826)]. Lom (1961) considered *A. marylandensis* as a valid species and recorded it rarely in *Allolobophora longa* [= *Aporrectodea longa* (Ude, 1885)] and *Dendrobaena octaedra* (Savigny, 1826). However, Lom (1961) did not list these two species in his comprehensive table but provided there two completely different earthworm species, *Octolasium lacteum* [= *Octolasion lacteum*] and *Allolobophora caliginosa* [= *Aporrectodea caliginosa*]. Due to the conflicts between text and tables, it is not possible to state where Lom (1961) detected *A. marylandensis*.

Heidenreich (1935) also considered *A. alluri* Cépède, 1910, *A. lloydii* Ghosh, 1918 and *A. striata* (Dujardin, 1841) as junior synonyms of *A. lumbrici*. In addition, he also found *A. striata* as synonyms of *A. alluri* and *A. nodulata*. According to Lom (1961), *A. alluri* is also a junior synonym of *A. nodulata*. Whether the two latter species are conspecific and also identical with *A. simplex* Nana *et al.*, 2018 is difficult to decide at the present state of knowledge. However, synonymization of *A. alluri* and *A. nodulata* with *A. lumbrici* is not justified in the light of both morphological (two rows of contractile vacuoles vs a single row of vacuoles) and molecular (Figs 14–15) data. Cépède (1910) discovered *Anoplophrya alluri* in *Allurus tetraedrus* [= *Eiseniella tetraedra* (Savigny, 1826)], but he provided a much wider host spectrum for *A. striata*: *L. rubellus*, *L. terrestris*, *L. variegatus* [= *Lumbriculus variegatus* (Müller, 1774)], *E. foetida* and *Al. chlorotica*. According to Ghosh (1918), *A. lloydii* originated from *Pheretima posthuma* [= *Perichaeta posthuma* Vaillant, 1868] which, however, does not belong to the family Lumbricidae but to the Megascolecidae. *Anoplophrya simplex* was isolated from *Alma emini* (Michaelsen, 1892) which belongs to the Glossoscolecidae (Nana *et al.* 2018). Therefore, conspecificity of *A. alluri*, *A. lloydii* and *A. simplex* is unlikely, although all three species display two rows of contractile vacuoles.

We detected *A. vulgaris* exclusively from the epigeic earthworms *E. fetida* and *D. veneta*. Ciliate 18S rRNA gene sequences obtained from both hosts were identical. Similarly, de Puytorac (1954, 1972), Lom (1961) and Paisán *et al.* (2009) reported *A. vulgaris* from epigeic earthworms. The third detected species of *Anoplophrya* in the present study was identified as *A. nodulata*. Heidenreich (1935) considered it incorrectly as a junior synonym of *A. lumbrici* (see above). Dujardin (1841) did not specify the host organism in which he discovered *A. nodulata*. We have detected it exclusively in a single endogeic species, *O. tyrtaeum*. Lom (1961) frequently recorded *A. nodulata* in *E. tetraedra* and rarely in *A. caliginosa*. Because of quite different host species, the conspecificity of our and Lom's (1961) populations is questionable and needs to be tested by molecular data.

According to the compendium of de Puytorac (1972), seven further species of *Anoplophrya* were reported from earthworms of the family Lumbricidae: (1) *Anoplophrya commune* de Puytorac, 1954 from *Allolobophora savignyi* [= *Scherotheca savignyi*]; (2) *Anoplophrya enigmatica* (authorship not provided by de Puytorac 1972) from *Dendrobaena subrubicunda* [= *Dendrodrilus rubidus subrubicundus*]; (3) *Anoplophrya oblonga* de Puytorac, 1954 from *L. herculeus* and *L. terrestris*; (4) *Anoplophrya problematica* (authorship not provided by de Puytorac 1972) from *Dendrobaena illyrica*; (5) *Anoplophrya singularis* de Puytorac, 1954 from *L. festivus* (Savigny, 1826); (6) *Anoplophrya suspicata* (authorship not provided by de Puytorac 1972) from *L. castaneus* (Savigny, 1826); and (7) *Anoplophrya tchadovi* de Puytorac, 1958 from "*Eiseniella ohridana* Cern" [= *E. tetraedra* var. *ochridana* Černosvitov, 1931].

The present phylogenetic analyses did not support monophylies of the genera *Metaracoelophrya*, *Metaradiophrya* and *Anoplophrya* (Figs 14–15). Monophyly of *Metaracoelophrya* was also firmly refuted by all statistical tree topology tests (Table 6). To solve this taxonomic problem, details on morphology of the three species of *Metaracoelophrya* are needed. Likewise, monophyly of *M. lumbrici*, *M. varians* and *Metaradiophrya* sp. HQ446279 was consistently rejected, although monophyly of *M. lumbrici* and *M. varians* could not be excluded by any statistical test (Table 6). However, examination of the dissertation thesis of Fokam (2012) revealed that *Metaradiophrya* sp. HQ446279 (= "*Metaradiophrya simplex*" in his thesis) is obviously not a *Metaradiophrya*, since it does not possess a fibrillar hook composed of two unequally long arms. Finally, polyphyly of the genus *Anoplophrya* is caused in that *A. nodulata* clusters far away from the *A. lumbrici* + *A. marylandensis* + *A. vulgaris* clade. As mentioned above, the genetic divergence of *A. nodulata* and the two other species of *Anoplophrya* is comparatively big (0.0717–0.0752) and even greater than from the two species of *Metaradiophrya* (0.0608–0.0627). Since *A. nodulata* is distinguished from the two other species of *Anoplophrya* by the contractile vacuole pattern (two rows vs one row) and by the ecological group of host earthworms (endogeic vs anecic or epigeic), it should be transferred to a distinct genus. However, due to the lack of detailed morphological data on *A. nodulata*, we prefer not to establish a new genus in the present study.

It is important to emphasize that all literature data on occurrence of astome ciliates in the digestive tract of oligochaetes from the family Lumbricidae are problematic due to taxonomic difficulties and lack of molecular data. Our integrative approach revealed that reliable identification of astome ciliates also requires molecular data. Moreover, our phylogenetic analyses also suggest that astome ciliates might be associated with certain ecological and systematic groups of their host organisms. Therefore, occurrence of individual astome species in ecologically different and phylogenetically distant earthworms seems to be unlikely and needs to be corroborated by molecular data.

Acknowledgements

We are grateful to Jaroslav Bella (Botanic Garden of Comenius University), Markéta Derdáková, Miroslav Obert, Jana Pazderová, Danica Smoláriková and Vladimír Vďačný for enabling us to sample in their gardens. This work was supported by the Slovak Research and Development Agency under the contract No. APVV-15-0147 and by the Grant Agency of the Ministry of Education, Science, Research and Sport of the Slovak Republic and Slovak Academy of Sciences under the Grants VEGA 1/0041/17 and VEGA 1/0114/16.

References

Abraham J.S., Sripoorna S., Maurya S., Makhija S., Gupta R. & Toteja R. 2019. Techniques and tools for species identification in ciliates: a review. *International Journal of Systematic and Evolutionary Microbiology* 69: 877–894. https://doi.org/10.1099/ijsem.0.003176

Affa'a F.-M., Hickey D.A., Strüder-Kypke M. & Lynn D.H. 2004. Phylogenetic position of species in the genera *Anoplophrya*, *Plagiotoma*, and *Nyctotheroides* (phylum Ciliophora), endosymbiotic ciliates of annelids and anurans. *Journal of Eukaryotic Microbiology* 51: 301–306. https://doi.org/10.1111/j.1550-7408.2004.tb00570.x

Beers C.D. 1938. Structure and division in the astomatous ciliate *Metaradiophrya asymmetrica* n. sp. *Journal of the Elisha Mitchell Scientific Society* 54: 111–125.

Bush M. 1933. The morphology of the ciliate *Haptophrya michiganensis* Woodhead and its relation to other members of the Astomatea. *Transactions of the American Microscopic Society* 52: 223–232. https://doi.org/10.2307/3222257

Bush M. 1934. The morphology of *Haptophrya michiganensis* Woodhead, an astomatous ciliate from the intestinal tract of *Hemidactylium scutatum* (Schlegel). *University of California Publications in Zoology* 39: 251–275.

Cépède C. 1910. Recherches sur les infusoires astomes. Anatomie, biologie, ethologie parasitaire, systématique. *Archives de Zoologie expérimentale et générale* 5: 341–609.

Conklin C. 1930. *Anoplophrya marylandensis* n. sp., a ciliate from the intestine of earthworms of the family Lumbricidæ. *Biological Bulletin* 58: 176–181. https://doi.org/10.2307/1536863

Corliss J.O., de Puytorac P. & Lom J. 1965. Resolution of persistent taxonomic and nomenclatural problems involving ciliate protozoa assignable to the astome family Haptophryidae Cepede, 1923. *Journal of Protozoology* 12: 265–273. https://doi.org/10.1111/j.1550-7408.1965.tb01849.x

Darriba D., Taboada G.L., Doallo R. & Posada D. 2012. jModelTest 2: more models, new heuristics and parallel computing. *Nature Methods* 9: 772. https://doi.org/10.1038/nmeth.2109

de Puytorac P. 1954. Contribution à l'étude cytologique et taxonomique les infusoires astomes. *Annales des Sciences naturalles, Zoologie et Biologie animale* 11: 85–270.

de Puytorac P. 1957. L'infraciliature de quelques ciliés Haptophryidae. Caparaison avec celle de certains thigmotriches. *Comptes Rendus hebdomadaires Séances de l'Académie des Sciences* 244: 1962–1965.

de Puytorac P. 1963. Contribution à l'étude des ciliés astomes Haptophryidae Cépède, 1903 (cytologie, ultrastructure, taxinomie). *Annales des Sciences naturelles, Zoologie et Biologie animale* 5: 173–210.

de Puytorac P. 1969. Les Ciliés Astomes Hoplitophryidae. I. Description de nouvelles espèces. *Protistologica* 5: 255–268.

de Puytorac P. 1972. Les Ciliés Astomes Hoplitophryidae. II. Révision de la systématique de ce groupe. *Protistologica* 8: 5–42.

de Puytorac P. & Schrével J. 1965. Nouvelles espèces de Ciliés Astomes endoparasites d'Annélides Polychètes. *Annales de la Faculte des Sciences de l'Universite de Clermont* 28: 85–99.

Dujardin F. 1841. *Histoire naturelle des zoophytes. Infusoires, comprenant la physiologie et la classification de ces animaux, et la maniére de les étudier a l'aide du microscope*. Librairie Encyclopédique de Roret, Paris.

Foissner W. 2014. An update of 'basic light and scanning electron microscopic methods for taxonomic studies of ciliated protozoa'. *International Journal of Systematic and Evolutionary Microbiology* 64: 271–292. https://doi.org/10.1099/ijs.0.057893-0

Fokam Z. 2012. *Etude morphologique et phylogénie des Ciliés Astomes endocommensaux d'Oligochètes terricoles de la région de Yaoundé et ses environs*. PhD thesis, *Université de Yaoundé I*, *Cameroon*.

Fokam Z., Nhassam P., Boutin C. & Togouet S.H.Z. 2008. Trois espèces nouvelles de *Coelophrya*, Ciliés Astomes endocommensaux d'*Alma nilotica* (oligochète terricole) du Cameroun. *Bulletin de la Société d'Histoire naturelle de Toulouse* 144: 27–33.

Fokam Z., Ngassam P., Strüder-Kypke M.C. & Lynn D.H. 2011. Genetic diversity and phylogenetic position of the subclass Astomatia (Ciliophora) based on a sampling of six genera from West African oligochaetes (Glossoscolecidae, Megascolecidae), including description of the new genus *Paraclausilocola* n. gen. *European Journal of Protistology* 47: 161–171. https://doi.org/10.1016/j.ejop.2011.02.002

Fokam Z., Nana P.A., Moche K., Bricheux G., Bouchard P., Ngassam P. & Sime-Ngando T. 2015. Influence of soil physicochemical parameters on the abundance of *Paracoelophrya polymorphus* (Ciliophora: Radiophryidae) commensal of earthworms (Annelida: Glossoscolecidae) collected in Bambui (North-West Cameroon). *Journal of Biodiversity and Environmental Sciences* 6: 376–389.

Fokam Z., Nana P.A., Bricheux G., Vigues B., Bouchard P., Ngassam P. & Sime-Ngando T. 2016. Correlation between some environmental variables and abundance of *Almophrya mediovacuolata* (Ciliophora: Anoplophryidae) endocommensal ciliate of an anecic earthworms (Oligochaeta: Annelida) in Bambui (North-West Cameroon). *International Journal of Biological and Chemical Sciences* 10: 1983–1997. https://doi.org/10.4314/ijbcs.v10i5.4

Ghosh E. 1918. Studies on Infusoria. *Records of the Indian Museum (Calcutta)* 15: 129–134.

Gower J.C. 1971. A general coefficient of similarity and some of its properties. *Biometrics* 27: 857–871. https://doi.org/10.2307/2528823

Guindon S., Dufayard J.F., Lefort V., Anisimova M., Hordijk W. & Gascuel O. 2010. New algorithms and methods to estimate maximum-likelihood phylogenies: assessing the performance of PhyML 3.0. *Systematic Biology* 59: 307–321. https://doi.org/10.1093/sysbio/syq010

Hall T.A. 1999. BioEdit: a user-friendly biological sequence alignment editor and analysis program for Windows 95/98/NT. *Nucleic Acids Symposium Series* 41: 95–98.

Heidenreich E. 1935. Untersuchungen an parasitischen Ciliaten aus Anneliden. Teil I: Systematik. *Archiv für Protistenkunde* 84: 315–392.

Hunter J.D. 2007. Matplotlib: a 2D graphics environment. *Computing in Science and Engineering* 9: 90–95.

Irwin N.A.T. & Lynn D.H. 2015. Molecular phylogeny of mobilid and sessilid ciliates symbiotic in eastern pacific limpets (Mollusca: Patellogastropoda). *Journal of Eukaryotic Microbiology* 62: 543–552. https://doi.org/10.1111/jeu.12208

Irwin N.A.T., Sabetrasekh M. & Lynn D.H. 2017. Diversification and phylogenetics of mobilid peritrichs (Ciliophora) with description of *Urceolaria parakorschelti* sp. nov. *Protist* 168: 481–493. https://doi.org/10.1016/j.protis.2017.07.003

Kay M.W. 1942. A new astomatous ciliate from the newt, *Eurycea bislineata* (Green). *American Midland Naturalist Journal* 27: 422–427.

Kijenskij G. 1926. Nálevníci zažívací roury některých Oligochaetů pražského okolí (Morfologie. Nepohlavní množení. Systematika). *Věstník Královské České Společnosti Nauk, Třída Matematicko-Přírodovědecká* year 1925 (I): 1–32.

Kumar S., Stecher G., Li M., Knyaz C. & Tamura K. 2018. MEGA X: Molecular Evolutionary Genetics Analysis across computing platforms. *Molecular Biology and Evolution* 35: 1547–1549. https://doi.org/10.1093/molbev/msy096

Lom J. 1959. Beiträge zur Kenntnis der parasitischen Ciliaten aus Evertebraten. IV Neue Ciliaten aus der Familie Haptophryidae Cépède 1923, nebst einigen Bemerkungen zum heutigen Stand dieser Gruppe. *Archiv für Protistenkunde* 104: 133–154.

Lom J. 1961. Some remarks on the morphology and taxonomy of astomatous ciliates from earthworms. *Acta Societatis Zoologicae Bohemoslovenicae* 25: 167–180.

Lynn D.H. 2008. *The Ciliated Protozoa. Characterization, Classification and Guide to the Literature*. 3rd ed. Springer, Dordrecht.

Maupas E. 1879. Sur l'*Haptophyra gigantea* opaline nouvelle de l'intestine des batraciens anoures d'Algérie. *Comptes Rendus hebdomadaires Séances de l'Académie des Sciences* 88: 921–923.

McAllister C.T. & Trauth S.E. 1996. Ultrastructure of *Cepedietta virginiensis* (Protista: Haptophryidae) from the gall bladder of the pickerel frog, *Rana palustris*, in Arkansas. *Proceedings of the Arkansas Academy of Science* 50: 133–136.

McAllister C.T., Upton S.J. & Trauth S.E. 1993. Endoparasites of western slimy salamanders, *Plethodon albagula* (Caudata: Plethodontidae), from Arkansas. *Journal of the Helminthological Society of Washington* 60: 124–126.

McKinney W. 2010. Data structures for statistical computing in Python. *In*: van der Walt S. & Millman J. (eds) *Proceedings of the 9th Python in Science Conference*: 51–56. Austin, Texas.

Medlin L., Elwood H.J., Stickel S. & Sogin M.L. 1988. The characterization of enzymatically amplified eukaryotic l6S-like rRNA-coding regions. *Gene* 71: 491–499.

Miller M.A., Pfeiffer W. & Schwartz T. 2010. Creating the CIPRES Science Gateway for inference of large phylogenetic trees. *In*: *Proceedings of the Gateway Computing Environments Workshop (GCE)*: 1–8. Piscataway, N.J., New Orleans, Louisiana.

Nana P.A., Fokam Z., Viguès B., Bricheux G., Aghaindum G.A., Ngassam P., Nola M. & Sime-Ngando T. 2018. Morphology and infraciliature of two new earthworm ciliates, *Hoplitophrya polymorphus* sp. nov. and *Anoplophrya simplex* sp. nov. (Ciliophora: Oligohymenophorea: Astomatia). *Zootaxa* 4392: 169–178. http://dx.doi.org/10.11646/zootaxa.4392.1.9

Ngassam P. 1983. Trois espèces nouvelles de ciliés Astomes des genres: *Almophrya* de Puytorac et Dragesco, 1968, *Maupasella* Cépède, 1910, *Njinella* nov. genre, endocommensaux d'Annélides oligochètes de la région de Yaoundé. *Protistologica* 19: 131–135.

Ngassam P., Fokam Z., Gangoué P.J. & Motchebe N.G.M. 1998. Complément à la connaissance de deux ciliés Astomes endocommensaux d'Oligochètes terricoles de la région de Yaoundé. *Cameroun Journal of Biological and Biochemical Sciences* 8: 17–30.

Oliphant T.E. 2015. *Guide to NumPy*. 2nd ed. Continuum Press, Austin, Texas.

Paisán L., Alonso P., Anadón R. & Alvarez S. 2009. Descripción y primera mención en España de cuatro especies de ciliados endobiontes de *Eisenia fetida* (Savigny, 1826) (Annelida, Oligochaeta, Lumbricidae). *Boletín de la Real Sociedad Española de Historia Natural, Sección Biológica* 103: 37–47.

Pedregosa F., Varoquaux G., Gramfort A., Michel V., Thirion B., Grisel O., Blondel M., Pettenhofer P., Weiss R., Dubourg V., Vanderplas J., Passos A., Cournaupeau D., Brucher M., Perrot M. & Duchesnay É. 2011. Scikit-learn: Machine Learning in Python. *Journal of Machine Learning Research* 12: 2825–2830.

Pižl V. 2002. Žížaly České republiky. *Sborník přírodovědného klubu v Uherskom Hradišti* Supplementum 9: 1–154.

Rataj M. & Vďačný P. 2018. Dawn of astome ciliates in light of morphology and time-calibrated phylogeny of *Haptophrya planariarum*, an obligate endosymbiont of freshwater turbellarians. *European Journal of Protistology* 64: 54–71. https://doi.org/10.1016/j.ejop.2018.03.004

Rataj M. & Vďačný P. 2019. Living morphology and molecular phylogeny of oligohymenophorean ciliates associated with freshwater turbellarians. *Diseases of Aquatic Organisms* 134: 147–166. https://doi.org/10.3354/dao03366

Ronquist F., Teslenko M., van der Mark P., Ayres D.L., Darling A., Höhna S., Larget B., Liu L., Suchard M.A. & Huelsenbeck J.P. 2012. MrBayes 3.2: efficient Bayesian phylogenetic inference and model choice across a large model space. *Systematic Biology* 61: 539–542. https://doi.org/10.1093/sysbio/sys029

Rossolimo L. 1926a. Parasitische Infusorien aus dem Baikalsee. *Archiv für Protistenkunde* 54: 468–510.

Rossolimo L. 1926b. Über einige neue und wenig bekannte Infusoria-Astomata aus den Anneliden des russischen Nordens. *Zoologischer Anzeiger* 68: 52–57.

Sauvadet A.L., Lynn D.H., Roussel E.G., Le Panse S., Bigeard E., Schrével J. & Guillou L. 2017. Redescription and phylogenetic analyses of *Durchoniella* spp. (Ciliophora, Astomatida) associated with the polychaete *Cirriformia tentaculata* (Montagu, 1808). *European Journal of Protistology* 61: 265–277. https://doi.org/10.1016/j.ejop.2017.06.007

Schneider C.A., Rasband W.S. & Eliceiri K.W. 2012. NIH Image to ImageJ: 25 years of image analysis. *Nature Methods* 9: 671–675. https://doi.org/10.1038/nmeth.2089

Schultze M.S. 1851. Beiträge zur Naturgeschichte der Turbellarien. C.A. Koch's Verlagshandlung, Greifswald.

Sela I., Ashkenazy H., Katoh K. & Pupko T. 2015. GUIDANCE2: accurate detection of unreliable alignment regions accounting for the uncertainty of multiple parameters. *Nucleic Acids Research* 43: W7–W14. https://doi.org/10.1093/nar/gkv318

Shimodaira H. 2002. An approximately unbiased test of phylogenetic tree selection. *Systematic Biology* 51: 492–508. https://doi.org/10.1080/10635150290069913

Shimodaira H. 2008. Testing regions with non-smooth boundaries via multiscale bootstrap. *Journal of Statistical Planning and Inference* 138: 1227–1241. https://doi.org/10.1016/j.jspi.2007.04.001

Shimodaira H. & Hasegawa M. 2001. CONSEL: for assessing the confidence of phylogenetic tree selection. *Bioinformatics* 17: 1246–1247. https://doi.org/10.1093/bioinformatics/17.12.1246

Sikora J. 1963. Study on the parasitic ciliate *Steinella uncinata* (Schultze). *Acta Protozoologica* 1: 13–20.

Swofford D.L. 2003. *PAUP*. Phylogenetic Analysis Using Parsimony (*And Other Methods)*. Version 4.0b 10. Sinauer Associates, Sunderland.

Tamura K. & Kumar S. 2002. Evolutionary distance estimation under heterogeneous substitution pattern among lineages. *Molecular Biology and Evolution* 19: 1727–1736. https://doi.org/10.1093/oxfordjournals.molbev.a003995

Vďačný P. 2018. Evolutionary associations of endosymbiotic ciliates shed light on the timing of the marsupial-placental split. *Molecular Biology and Evolution* 35: 1757–1769. https://doi.org/10.1093/molbev/msy071

Vďačný P., Érseková E., Šoltys K., Budiš J., Pecina L. & Rurik I. 2018. Co-existence of multiple bacterivorous clevelandellid ciliate species in hindgut of wood-feeding cockroaches in light of their prokaryotic consortium. *Scientific Reports* 8: 17749. https://doi.org/10.1038/s41598-018-36245-y

Vďačný P., Rajter Ľ., Stoeck T. & Foissner W. 2019. A proposed timescale for the evolution of armophorean ciliates: clevelandellids diversify more rapidly than metopids. *Journal of Eukaryotic Microbiology* 66: 167–181. https://doi.org/10.1111/jeu.12641

von Siebold C.T. 1839. Beiträge zur Naturgeschichte der wirbellosen Thiere. Ueber Medusa, Cyclops, Loligo, Gregarina und Xenos. Neueste Schriften der Naturforschenden Gesellschaft in Danzig, Vol 3. Fr. Sam. Gerhard, Danzig.

Williams G.W. 1942. Observations on several species of *Metaradiophrya* (Protozoa, Ciliata). *Journal of Morphology* 70: 545–589.

Manuscript received: 13 May 2019
Manuscript accepted: 15 July 2019
Published on: 1 October 2019
Topic editor: Rudy Jocqué
Desk editor: Eva-Maria Levermann